

# Western European Land Use Regression Incorporating Satellite- and Ground-Based Measurements of NO<sub>2</sub> and PM<sub>10</sub>

Danielle Vienneau,<sup>\*,†,‡,§</sup> Kees de Hoogh,<sup>§</sup> Matthew J. Bechle,<sup>||</sup> Rob Beelen,<sup>⊥</sup> Aaron van Donkelaar,<sup>#</sup> Randall V. Martin,<sup>#,▲</sup> Dylan B. Millet,<sup>||</sup> Gerard Hoek,<sup>⊥</sup> and Julian D. Marshall<sup>||</sup>

<sup>†</sup>Department of Epidemiology and Public Health, Swiss Tropical and Public Health Institute, 4051, Basel, Switzerland

<sup>‡</sup>University of Basel, 4003, Basel, Switzerland

<sup>§</sup>MRC-PHE Centre for Environment and Health, Department of Epidemiology and Biostatistics, Imperial College London, London SW7 2AZ, United Kingdom

<sup>||</sup>Department of Civil Engineering, University of Minnesota, Minneapolis, Minnesota 55455, United States

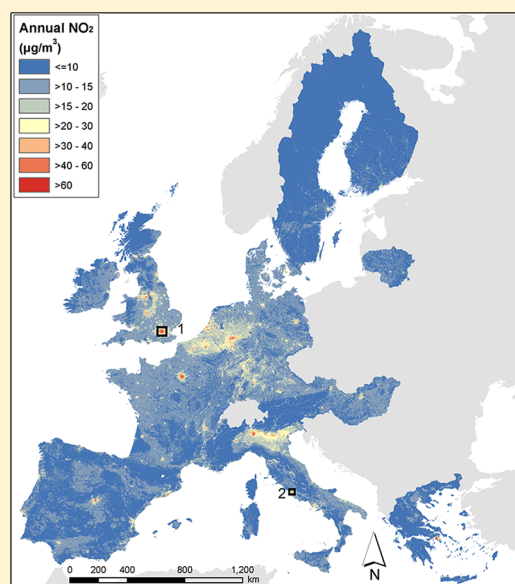
<sup>⊥</sup>Institute for Risk Assessment Sciences, Division Environmental Epidemiology, Utrecht University, 3512 JE Utrecht, The Netherlands

<sup>#</sup>Department of Physics and Atmospheric Science, Dalhousie University, Halifax, Nova Scotia, B3H 4R2, Canada

<sup>▲</sup>Harvard-Smithsonian Center for Astrophysics, Cambridge, Massachusetts 02138, United States

## **S** Supporting Information

**ABSTRACT:** Land use regression (LUR) models typically investigate within-urban variability in air pollution. Recent improvements in data quality and availability, including satellite-derived pollutant measurements, support fine-scale LUR modeling for larger areas. Here, we describe NO<sub>2</sub> and PM<sub>10</sub> LUR models for Western Europe (years: 2005–2007) based on >1500 EuroAirnet monitoring sites covering background, industrial, and traffic environments. Predictor variables include land use characteristics, population density, and length of major and minor roads in zones from 0.1 km to 10 km, altitude, and distance to sea. We explore models with and without satellite-based NO<sub>2</sub> and PM<sub>2.5</sub> as predictor variables, and we compare two available land cover data sets (global; European). Model performance (adjusted R<sup>2</sup>) is 0.48–0.58 for NO<sub>2</sub> and 0.22–0.50 for PM<sub>10</sub>. Inclusion of satellite data improved model performance (adjusted R<sup>2</sup>) by, on average, 0.05 for NO<sub>2</sub> and 0.11 for PM<sub>10</sub>. Models were applied on a 100 m grid across Western Europe; to support future research, these data sets are publicly available.



## 1. INTRODUCTION

Land use regression (LUR) has rapidly become a standard approach for estimating spatial variability in air pollution, for example during exposure assessment in epidemiological studies. Since the inception of LUR,<sup>1</sup> many studies have explored how well LUR can estimate within-city spatial variability in pollutant concentrations.<sup>2,3</sup> Recent attention has focused on comparing LUR to other methods such as interpolation and dispersion modeling,<sup>4,5</sup> applying LUR to specific constituents (e.g., soot) and elements of PM<sub>2.5</sub><sup>6,7</sup> and specific organic compounds (e.g., PAHs);<sup>3,8</sup> and evaluating the transferability of models to other spatial and temporal contexts.<sup>9–14</sup>

LUR models are often derived from measurements made specifically to build the LUR. An alternative approach is to

employ data from existing monitors; this approach is well suited to modeling broad geographic extents. Examples include individual European countries,<sup>11,15</sup> continental USA,<sup>16,17</sup> Canada,<sup>18</sup> and Western Europe.<sup>19</sup>

Here we develop NO<sub>2</sub> and PM<sub>10</sub> LUR models for Western Europe. Only one Europe-wide LUR has previously been published.<sup>19</sup> We improve on that investigation by offering 2 orders of magnitude improvement in spatial resolution (1 km<sup>2</sup> [prior<sup>19</sup>] versus 0.01 km<sup>2</sup> [here]) and by including

**Received:** July 12, 2013

**Revised:** October 20, 2013

**Accepted:** October 24, 2013

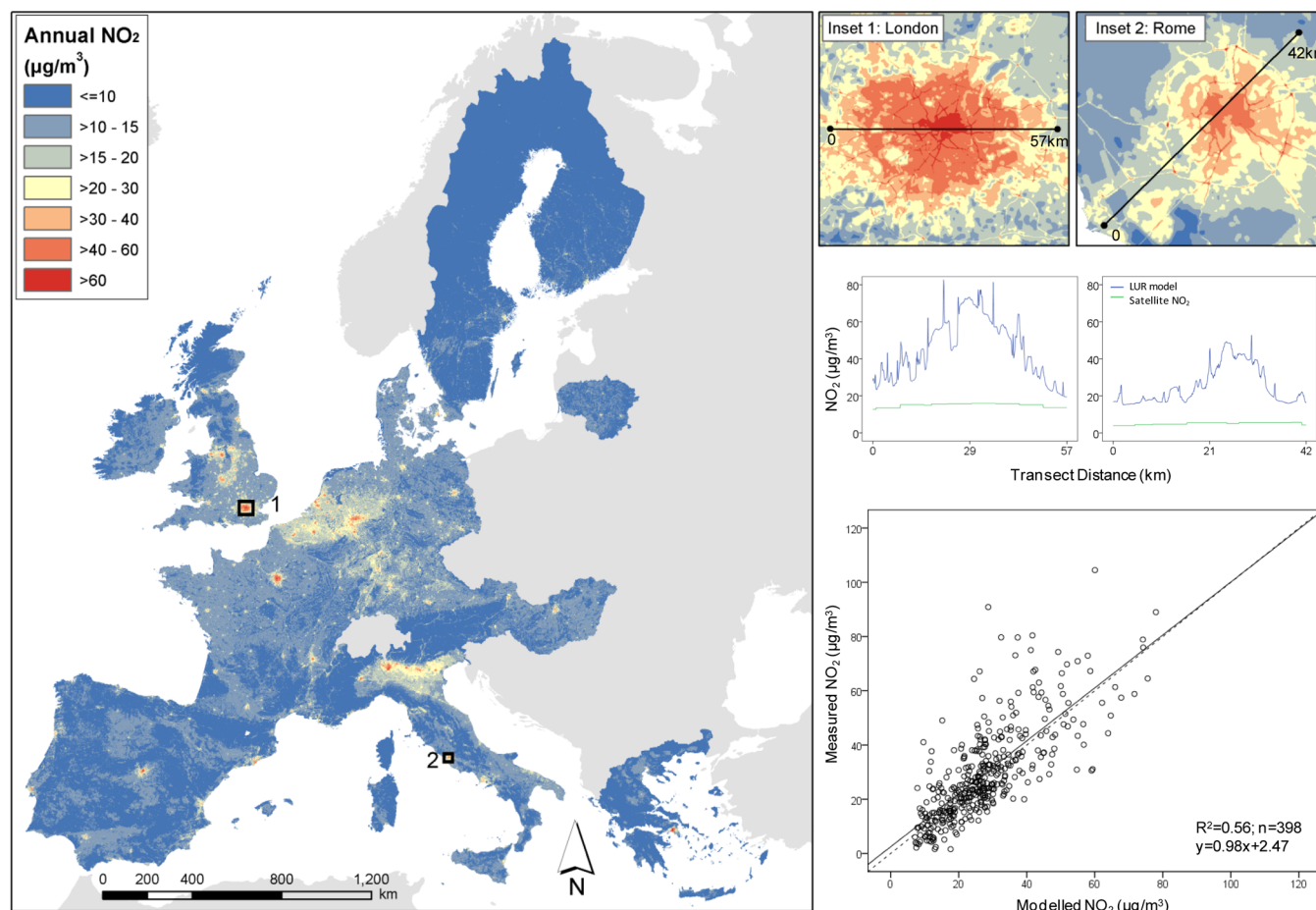


Figure 1. Map and profile plots of NO<sub>2</sub> concentration in 2005 using satellite data; scatterplot of modeled vs measured NO<sub>2</sub> at evaluation sites.

Table 1. Summary Statistics for Mean Annual Concentrations (µg/m<sup>3</sup>) at All Monitoring Sites with ≥75% Annual Data Capture<sup>a</sup>

year	N	min	5%	95%	max	mean	SD	GM	GSD
NO <sub>2</sub>									
2005	2010	0.8	7.1	60.8	112.3	29.3	16.5	24.5	1.9
2006	2099	0.9	7.9	61.8	121.3	29.8	16.8	25.1	1.9
2007	2236	0.3	7.5	58.7	106.5	28.8	15.9	24.3	1.9
2005–2007	1670	0.9	8.0	57.9	108.5	28.5	15.5	24.2	1.9
PM <sub>10</sub>									
2005	1487	7.8	14.8	44.9	70.9	26.6	9.2	25.2	1.4
2006	1584	7.7	15.7	45.7	71.7	27.7	9.2	26.3	1.4
2007	1664	3.6	15.2	44.1	77.4	26.7	8.7	25.4	1.4
2005–2007	1151	7.7	16.1	43.5	61.7	26.7	8.3	25.5	1.4

<sup>a</sup>GM = geometric mean; GSD = geometric standard deviation (unit less).

satellite-derived estimates of ground-level air pollution. Investigations with large populations and geographic extents, including epidemiological studies of air pollution and traffic-related air pollution, environmental injustice studies, and health risk assessment, would benefit from continental-scale models with a finer spatial resolution.

We investigate whether satellite-derived pollution measurements improve fine-scale concentration estimates in European-wide LURs. Our approach incorporates GIS-derived land use, topographic data, and satellite-derived estimates of ground-level concentrations for NO<sub>2</sub> and PM<sub>2.5</sub>. We benefit from the large number of regulatory monitoring stations (EuroAirnet)

operating in Western Europe, facilitating independent evaluation with reserved sites.

## 2. METHODS

We develop land use regression (LUR) models for Western Europe (17 contiguous countries; Figure 1). Our dependent variables are ambient concentrations of NO<sub>2</sub> and PM<sub>10</sub>, obtained from regulatory monitoring. Our independent variables include several GIS-derived measures of land use and topography (100 m grids) and satellite-derived estimates of surface concentrations of NO<sub>2</sub> and PM<sub>2.5</sub> (not PM<sub>10</sub>; despite the availability of satellite-derived PM<sub>2.5</sub> estimates, there is an insufficient number of ground-based monitoring sites to

Table 2. GIS Predictor Variables

data set	variable <sup>a</sup>	code	buffer <sup>b</sup> or point estimate
OMI derived NO <sub>2</sub> (ppb): ~10 km	surface NO <sub>2</sub> concentration	SNO2	point
Terra derived PM <sub>2.5</sub> (μg/m <sup>3</sup> ): ~10 km	surface PM <sub>2.5</sub> concentration	SPM	point
Corine land cover <sup>c</sup> (% area)	continuous urban fabric - high density	Hdr	buffer
	discontinuous urban fabric - low density	Ldr	
	industry	Ind	
	ports	Port	
	urban green	Urbgr	
	total built up (Res + Ind + Port + transport infrastructure, airports, mines, dumps and construction sites)	Tbu	
	seminatural land	Nat	
	residential (Hdr + Ldr)	Res	
global land cover (% area)	impervious surface	Isurf	buffer
	tree canopy	Tree	
EuroStreets roads (length in m)	major roads	Majrd	buffer
	minor roads	Minrd	
modeled population (N)	population	Pop	buffer
topography: 90 m SRTM DTM	altitude - transformed <sup>d</sup>	Talt	point
modeled distance to sea (m)	distance to sea - transformed <sup>e</sup>	Tsea	point
coordinates (m)	XY coordinates for 100 m cell centroids	Xcoord	point
		Ycoord	

<sup>a</sup>Prespecified direction of effect is negative for: Urbgr, Nat, Tree, Talt, and Ycoord for both pollutants; and Tsea for PM<sub>10</sub>. <sup>b</sup>“Buffer” zone distances (m): 0; 100; 200; 300; 400; 500; 600; 700; 800; 1000; 1200; 1500; 1800; 2000; 2500; 3000; 3500; 4000; 5000; 6000; 7000; 8000; 10000. <sup>c</sup>Original Corine classes: Hdr: class 111; Ldr: class 112; Ind: class 121; Port: class 123; Urbgr: class 141–142; Tbu: class 111–133; Nat: class 311–423; Res: class 111–112. <sup>d</sup>Transformed altitude is calculated as  $\sqrt{(\text{nalt}/\text{max}(\text{nalt}))}$ , where nalt = altitude - min(altitude). <sup>e</sup>Transformed distance to sea is calculated as  $\sqrt{(\text{minimum distance}/\text{max}(\text{minimum distance}))}$ .

support modeling PM<sub>2.5</sub>). We next describe the input data and then our modeling approach.

**2.1. Data. 2.1.1. Ground-Based Monitoring Data.** We use annual mean NO<sub>2</sub> and PM<sub>10</sub> concentrations (years 2005–2007) from EuroAirnet, the regulatory air pollution monitoring network in Europe. EuroAirnet comprises sites from national networks<sup>20</sup> and is publicly reported in AirBase (version 5).<sup>21</sup> NO<sub>2</sub> is monitored by chemiluminescence. PM<sub>10</sub> is monitored by various methods including Tapered Element Oscillating Microbalance (TEOM), Beta Attenuation, and Gravimetric methods.<sup>22</sup> The network includes “background”, “industrial”, and “traffic” sites; all site types are included here. Urban background sites are representative of the exposure of the general urban population while rural background are sited away from major sources of air pollution.<sup>23</sup> Annual measurements are excluded if a site captured <75% of the total hours (NO<sub>2</sub>) or days (PM<sub>10</sub>). Table 1 presents summary statistics for retained monitoring sites. For each year, monitoring data are randomly stratified (by country and site type) into five groups, each with 20% of sites. Subset 1 (20%) is used for model evaluation; the remaining four subsets (80%) are combined and used for model building. As a sensitivity analysis, we apply a 5-fold cross-validation procedure in which the 20% evaluation subset is rotated, thereby creating four additional models. We *a priori* designate the first subset to model evaluation, reverting to the next subset only if spatial autocorrelation is detected. We further evaluate models developed using 100% of the monitoring sites and undertake a sensitivity analysis including country to investigate potential differences in the national networks comprising AirBase.

**2.1.2. Satellite-Derived Estimates of Ground-Level Concentrations.** We employ satellite-derived estimates of ground-level NO<sub>2</sub><sup>17</sup> and PM<sub>2.5</sub>.<sup>24</sup> Tropospheric NO<sub>2</sub> columns are from

the OMI (Ozone Monitoring Instrument) instrument onboard the Aura satellite.<sup>25</sup> Aerosol optical depth (AOD) retrieved from the MODIS (Moderate Resolution Imaging Spectroradiometer)<sup>26</sup> and MISR (Multiangle Imaging Spectroradiometer)<sup>27</sup> instruments onboard the Terra satellite is used to estimate PM<sub>2.5</sub>. As described elsewhere,<sup>17,24,28</sup> satellite column-integrated retrievals were related to surface concentrations at 0.1° × 0.1° resolution (~10 km grid) using scaling factors interpolated from the GEOS-Chem chemical transport model (www.geos-chem.org) that account for the local vertical distribution and scattering properties of each pollutant. Annual satellite-derived estimates for NO<sub>2</sub> were made for years 2005, 2006, and 2007. Satellite-derived humidity-corrected PM<sub>2.5</sub> estimates for 2001–2006 were aggregated to improve accuracy by enabling sufficient data capture; estimates for grid cells with <50 daily AOD measurements over the 6 years were removed.<sup>24</sup> In Europe, PM<sub>2.5</sub> represents a large fraction (40–80%) of PM<sub>10</sub> mass in ambient air,<sup>29,30</sup> motivating the use of satellite-derived PM<sub>2.5</sub> as an independent variable in a PM<sub>10</sub> LUR.

**2.1.3. Predictor Variables.** Predictor variables are integrated into a 100 m raster GIS database using ArcGIS10, employing the European reference grid (ETRS Lambert Azimuthal Equal Area S2 10). Satellite-derived pollution measurements and global land cover data are first resampled using nearest neighbor assignment; altitude is resampled using bilinear interpolation (used for continuous data). Variables, described below, are computed either as point estimates or zones. Zones of increasing radius (hereafter referred to as “buffers”) from 0.1 km to 10 km are computed using the Focalsum command with the circle option. Table 2 summarizes the predictor variables.

Two land cover data sets are available: the 100 m European Corine Land Cover<sup>31</sup> and coarser global data sets including 500 m tree canopy<sup>32</sup> and 1 km impervious surfaces.<sup>33</sup> On the

basis of the 44 land classes available in Corine, we define six main groups, represented by individual classes (Hdr, Ldr, Ind, Port; see Table 2) or aggregations of classes (Urbgr, Nat). We define two additional classes based on further aggregation of the urban classes (Res, Tbu). For both data sets (European; global), the percent area within in each buffer is computed for each land cover category. Population counts per grid cell are based on the European Environment Agency 1 km<sup>2</sup> population density grid.<sup>34,35</sup>

We use the 1:10,000 EuroStreets digital road network (version 3.1, based on TeleAtlas MultiNet TM for year-2008) to derive road density variables. EuroStreets includes 9 road classes, which we aggregate into major roads (motorways, main roads, and other major roads) and minor roads (secondary and four types of local roads). Nonmotorized tracks and paths are excluded. We intersect the road data with a 100 m base polygon and then calculate total length per grid cell and for each buffer. Consistent traffic-volume data are not available for Europe.

We use altitude data from the SRTM Digital Elevation Database version 4.1.<sup>36</sup> The resolution of the SRTM data is 3 arc second (approximately 90 m), with vertical error <16 m. SRTM is available for most of the study area, up to 60°N latitude. For northern Scandinavia we use 1 km resolution Topo30 data. Distance to sea, a measure of continentality, differentiates coastal from inland areas which are not, for example, influenced by coastal recirculation patterns and particulates from sea spray. We compute this variable as the distance between centroids of a 1 km grid and the open ocean 25 km offshore as defined by Corine land cover. Distance (in m) is then assigned to the 100 m grid using inverse distance weighed (1/d) interpolation. Interpolated distance was validated against direct calculation of distance to sea, using NEAR, at the monitoring sites ( $r = 99$ ). Following Beelen et al.,<sup>19</sup> we apply a nonlinear transformation to altitude and distance to sea (see Table 2). We also include X and Y coordinates for the cell centroids to reflect broad scale trends in background air pollution concentrations.<sup>9,11</sup>

**2.2. Modeling Approach.** LUR model development follows the ESCAPE supervised stepwise selection to derive the multiple linear regression equation.<sup>37,38</sup> Monitoring data (dependent variable), which are log-normally distributed, are log-transformed prior to modeling. We exclude potential predictor variables with  $\geq 90\%$  null values. Univariate regressions of the natural logarithm (LN) of annual mean concentrations and all available potential predictors variables are first developed, and the predictor with the highest adjusted  $R^2$  retained. In subsequent steps, the remaining predictor variables are evaluated in turn; the variable offering the highest increase in adj- $R^2$  is retained if (1) the coefficient conforms to the prespecified direction of effect (see Table 2), (2) each additional predictor variable increases the adj- $R^2$  by at least 0.01, and (3) the direction of effect for predictors already included in the model does not change. *Post hoc*, variables with  $p$ -value  $> 0.10$  or variance inflation factor (VIF)  $> 5$  are removed.<sup>17</sup> When required, *post hoc* “ring” (i.e., annulus) variables are calculated by differencing the component buffers, and the model is rerun to derive the final coefficients.<sup>11,38</sup> We apply standard diagnostic tests for ordinary least-squares regression, including checks on the normality of residuals, heteroscedasticity, spatial autocorrelation of residuals using Moran’s I, and influential observations using Cook’s D.

For models testing the inclusion of satellite-based measurements, that predictor variable is forced into the model as the

first variable, and the model is built according to the procedure above. Partial  $R^2$  values are recomputed and reported after the final model is derived. Models are evaluated against the independent subset of 20% sites reserved for this purpose;  $R^2$ , root mean squared error (RMSE), error, and bias<sup>17</sup> are reported here.

### 3. RESULTS

**3.1. Measured Concentrations from Ground-Based Monitoring.** Variability in annual mean NO<sub>2</sub> and PM<sub>10</sub> concentrations measured at the Airbase monitoring sites is relatively consistent across the three years (Table 1). For both pollutants, the number of sites available for modeling ( $\geq 75\%$  annual data capture) increases each year, owing to network growth, improvements in data capture, or both. The number of sites measuring continuously over the 3-year period is lower than the number of sites for any individual year (23% [17%] less for NO<sub>2</sub> [PM<sub>10</sub>], relative to 2005). Given the longer temporal period of the PM<sub>2.5</sub> satellite data, we also include LUR models based on the 3-year average concentrations. For both pollutants, the largest share of monitoring sites, with  $\sim 100$ –400 each, are in Austria, Italy, Spain, Germany, and France (see Supplementary Table S1). Most countries have either a consistent number or experienced an increase in number of sites by year. Great Britain is an exception, with a 60% (30%) reduction in NO<sub>2</sub> (PM<sub>10</sub>) site number in year-2007 relative to 2006. Spain also exhibits a dip in monitor numbers for both pollutants in 2006. Expansion in the network is greatest for Italy, with a 65% (86%) increase in NO<sub>2</sub> (PM<sub>10</sub>) sites from 2005 to 2007. For both pollutants, Pearson’s correlation between the ground- and satellite-based measurements ranges from 0.33–0.37. The agreement between observed PM<sub>10</sub> and satellite-derived PM<sub>2.5</sub> is likely decreased by differences in sampling period, spatial representation, and aerosol size but is sufficient to suggest applicability as a LUR predictor. Correlation is higher with background sites, which are expected to be more representative of the larger area covered by each satellite grid cell. Scatterplots are in Supplementary Figures S1 and S2.

**3.2. Model Comparison.** Table 3 compares the models on the basis of coefficient of determination ( $R^2$ ), mean error, and bias. For both pollutants, models with satellite data outperformed the respective model without satellite data, achieving higher model building and evaluation  $R^2$  and lower error and bias. Increases in adj- $R^2$  attributable to including satellite estimates are 0.02–0.06 for NO<sub>2</sub> and 0.07–0.13 for PM<sub>10</sub>. Selection of land cover data set (Corine vs global) yielded modest (at most 0.04) impacts to adj- $R^2$ .

The addition of satellite data did not substantially alter the structure of the NO<sub>2</sub> models (Table 3): road and land cover variables remain largely unchanged; other variables (altitude, population density, and distance to sea) only enter the models when satellite data is not included. By comparison, the PM<sub>10</sub> model structure is less stable both across and within years; a consistent pattern in variables entering models with and without satellite data is not apparent.

Model results are mapped in Figures 1 and 2 (models with satellite-derived pollution estimates) and Figures S3 and S4 (models without satellite-derived pollution estimates). For both pollutants, the models generally resolve expected patterns in air pollution, with higher concentrations in urban areas and near roadways. There are detectable differences, however, in the specific spatial patterns for cities (see map insets and profiles),

Table 3. Comparison of All Models<sup>d</sup>

year	model	with satellite					without satellite									
		model <sup>a</sup>		evaluation <sup>b</sup>			model <sup>a</sup>		evaluation <sup>b</sup>							
		variables <sup>c</sup>	Adj-R <sup>2</sup>	R <sup>2</sup>	ME	MAE	MB	MAB	variables <sup>c</sup>	Adj-R <sup>2</sup>	R <sup>2</sup>	ME	MAE	MB	MAB	
NO <sub>2</sub> Models	2005	Corine	SNO2-05, Minrd-1800, Nat-600, Majrd-100, Tbu-300, Minrd-1800-10000	0.58	0.56	-1.8	8.1	13	37	Tbu-2000, Minrd-400-10000, Nat-600, Majrd-100, Minrd-400	0.55	0.54	-1.7	8.8	16	42
		Global	SNO2-05, Minrd-400-1800, Majrd-100, Tree-300, Minrd-400, Isurf-800	0.56	0.57	-1.6	8.0	13	37	Minrd-500-2500, Majrd-100, Tree-700, Minrd-2500-10000, Minrd-500	0.51	0.51	-1.6	9.1	18	44
		Corine	SNO2-06, Minrd-1500, Majrd-100, Nat-500, Minrd-1500-10000, Tbu-300	0.55	0.50	-1.5	8.3	11	35	Tbu-1500, Minrd-100-10000, Nat-500, Majrd-100, Minrd-100, Pop-1000	0.53	0.47	-1.6	8.5	11	36
2006	Global	SNO2-06, Minrd-200-1500, Majrd-100, Isurf-500, Minrd-200, Tree-700	0.54	0.50	-1.0	8.3	13	36	Majrd-100, Minrd-200, Minrd-200-10000, Tree-700, Isurf-500, Tsea	0.49	0.46	-1.1	8.9	14	39	
	Corine	SNO2-07, Minrd-1500, Majrd-100, Nat-600, Tbu-300, Minrd-1500-10000	0.55	0.50	-1.3	8.5	18	41	Tbu-1200, Minrd-200-10000, Nat-600, Majrd-100, Minrd-200	0.51	0.48	-1.6	8.8	19	43	
2005-2007	Global	SNO2-07, Minrd-300-1500, Majrd-100, Tree-500, Minrd-300, Isurf-700	0.54	0.54	-1.4	8.1	20	43	Minrd-400-2500, Majrd-100, Tree-800, Minrd-2500-10000, Minrd-400, Talt, Tsea	0.48	0.46	-1.8	9.1	23	49	
	Corine	SNO2-05-07, Minrd-1500, Nat-600, Majrd-100, Minrd-1500-10000, Tbu-300	0.60	0.46	-1.8	8.4	8	34	Tbu-2000, Minrd-200-10000, Nat-600, Majrd-100, Minrd-200	0.56	0.48	-1.8	8.3	10	35	
PM <sub>10</sub> Models	2005	Global	SNO2-05-07, Minrd-400-1500, Majrd-100, Tree-700, Isurf-500, Minrd-400	0.58	0.50	-1.5	8.0	11	34	Minrd-500-2500, Majrd-100, Tree-800, Minrd-2500-10000, Minrd-500	0.52	0.41	-1.2	8.6	14	38
		Corine	SPM, Ycoord, Hdr-1200, Nat-500, Ind-100, Tsea	0.35	0.37	-0.7	5.7	5	22	Ycoord, Tbu-10000, Nat-1000	0.22	0.25	-1.1	6.1	4	23
2006	Global	SPM, Ycoord, Isurf-1000, Tree-500, Tsea, Majrd	0.35	0.44	-0.8	5.4	4	21	Tree-800, Ycoord, Isurf-1000-10000, Isurf-1000	0.22	0.25	-1.1	6.0	4	23	
	Corine	SPM, Ycoord, Tbu-600, Pop-1800, Tsea, Majrd-100, Nat-600	0.37	0.36	-1.2	6.0	3	22	Pop-1800, Ycoord, Nat-1000, Talt, Majrd-100, Ldr-10000	0.25	0.25	-1.9	6.4	1	23	
2007	Global	SPM, Ycoord, Isurf-800, Tree-100, Majrd-100	0.36	0.35	-1.5	6.0	2	22	Tree-1000, Ycoord, Isurf-1000, Majrd-100, Talt	0.24	0.20	-1.8	6.6	2	24	
	Corine	SPM, Ycoord, Minrd-2500, Talt, Tbu-100	0.49	0.45	-0.6	4.8	3	18	Ycoord, Nat-2000, Minrd-10000, Tbu-100, Talt, Majrd	0.42	0.36	-0.5	5.2	4	19	
2005-2007	Global	SPM, Ycoord, Minrd-200-2500, Talt, Minrd-200, Majrd, Tree-100	0.50	0.47	-0.5	4.6	4	17	Tree-1200, Ycoord, Minrd-200-6000, Talt, Minrd-200, Majrd-100	0.40	0.37	-0.8	5.1	3	19	
	Corine	SPM, Ycoord, Nat-1200, Tsea, Pop-1800, Tbu-400, Majrd-100	0.48	0.48	-0.2	4.4	3	17	Nat-2000, Ycoord, Tbu-300-10000, Talt, Tbu-300	0.36	0.31	-0.2	4.4	3	17	
2005-2007	Global	SPM, Ycoord, Isurf-200, Tree-600, Tsea, Majrd-100	0.48	0.48	-0.3	4.4	3	17	Tree-1000, Ycoord, Minrd-10000, Talt, Majrd-100	0.36	0.34	-0.8	4.9	3	18	

<sup>a</sup>Model building using natural logarithm of concentration (LN concentration). <sup>b</sup>Model evaluation using concentration ( $\mu\text{g}/\text{m}^3$ ); ME = mean error ( $\mu\text{g}/\text{m}^3$ ); MAE = mean absolute error ( $\mu\text{g}/\text{m}^3$ ); MB = mean bias (%); MAB = mean absolute bias (%). <sup>c</sup>Variables listed by order of entry into models, with satellite forced into the model as the first variable. <sup>d</sup>The best models are shown in boldface.

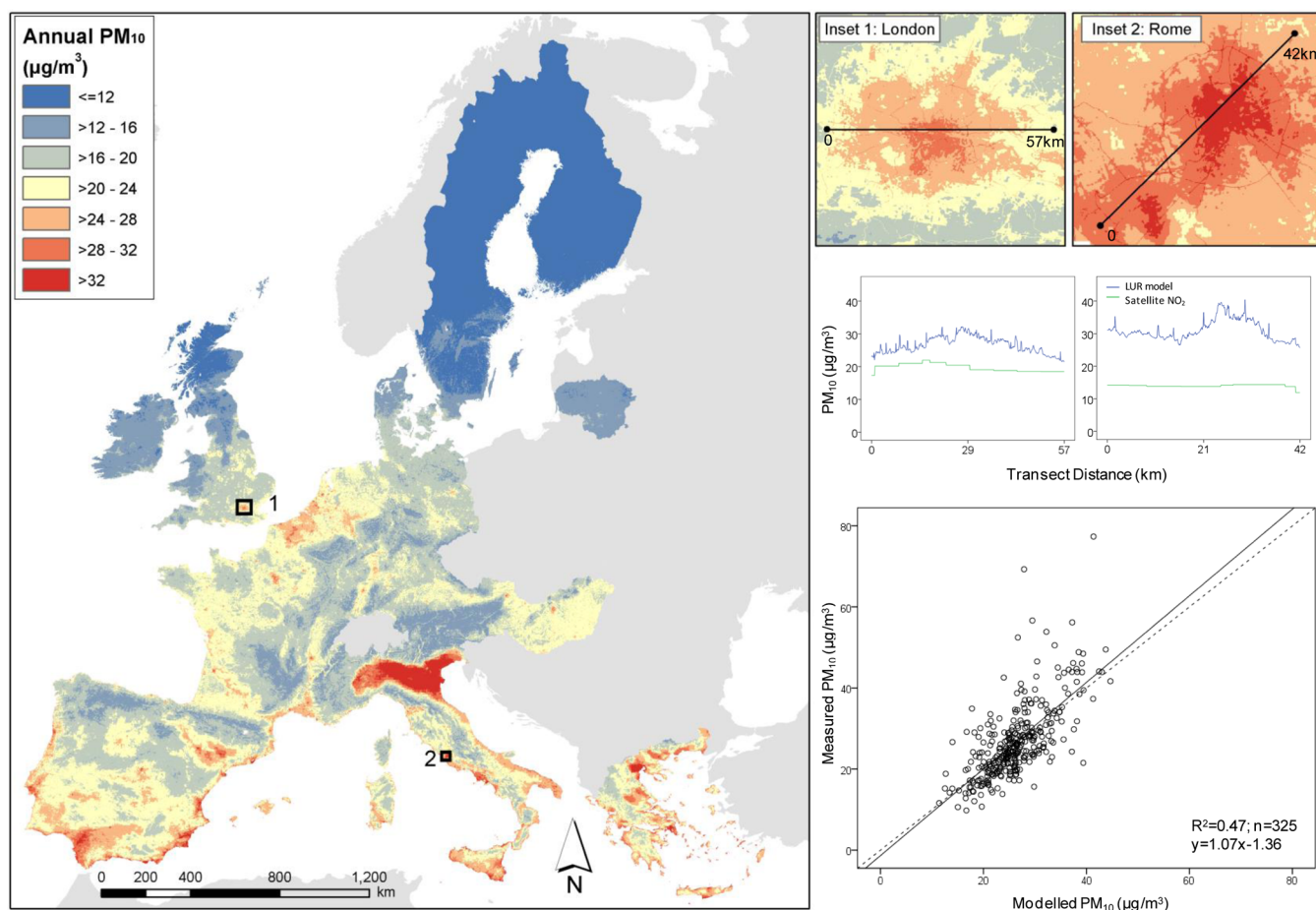


**Figure 2.** Map and profile plots of  $PM_{10}$  concentration in 2007 using satellite data; scatterplot of modeled vs measured  $PM_{10}$  at evaluation sites.

because of differences in the overall structure of the models. At the European scale, the maps show that known hotspots with frequently elevated regional background levels (e.g., the Ruhr area, Po valley, and western Netherlands) are better captured in models that include satellite-derived pollution estimates. Table S2 presents model evaluation by region. A striking example from that table is for the Italy + Greece region ( $PM_{10}$ ,  $n = 309$  monitors),  $R^2$  is 0.07 without satellite data, 0.45 with satellite data.

The sensitivity analysis of 80:20 subsets for annual models reveals that models are robust to changes in the evaluation subset; differences in adj- $R^2$  are slight ( $<0.02$  for  $NO_2$  and  $<0.04$  for  $PM_{10}$ ; see Table S3). Table S3 also shows the evaluation subset used to derive the models presented in Table 3. All models, for both pollutants, show no spatial autocorrelation in the residuals. Models based on 100% sites were similar in structure and performance (Tables S4 and S5). Including country indicators generally improved models, although not all indicators were statistically significant. Furthermore, to avoid the introduction of step changes in concentrations at country borders, we do not use country in our final models. Improvement was marked, up to  $\sim 20\%$ , for some of the  $PM_{10}$  models. This improvement, in part, is likely attributed to differences in PM monitoring equipment and may also reflect differences in calibration<sup>22</sup> and of site selection of the various countries.

**3.3. Final Models.**  $NO_2$ . The best-performing  $NO_2$  models by year are in Table S6. The variables in each  $NO_2$  model are consistent across years: in addition to satellite-derived surface  $NO_2$ , all models include the length of minor roads in an intermediate buffer (1500 or 1800 m) and in the outer ring to

10 km, major road length in a 100 m buffer, and total built up land from Corine in a 300 m buffer. The models also all contain Corine seminatural land with a negative coefficient in a 500 or 600 m buffer. Minor roads in the intermediate buffer contribute 59–65% to the model predictive power (partial  $R^2$ : 0.3–0.4), followed by satellite-based  $NO_2$  at 17–23% (partial  $R^2$ : 0.1). Those findings underscore the utility of satellite-based  $NO_2$  concentrations for  $NO_2$  LUR.

Overall, the final  $NO_2$  models explain 55–60% of the variation in log-transformed  $NO_2$  at the more than 400 reserved evaluation sites distributed across Europe (Table S8; Figure S5). Expressed and mapped as concentrations ( $\mu g/m^3$ ), the explained variation is 50–56%. Error and bias are relatively similar across years, with highest error + bias in year-2007: error ( $-1.3 - -1.8 \mu g/m^3$ ); absolute error ( $8.1-8.5 \mu g/m^3$ ); mean bias (11–18%); and absolute bias (34–41%). Minor road length and satellite estimates of  $NO_2$  are consistently the two most important predictors.

$PM_{10}$ . The best-performing model for  $PM_{10}$  by year is shown in Table S7. The variables in the final  $PM_{10}$  models varied by year, with the global land cover models performing better than Corine in 2005 and 2007. All models contain satellite-based  $PM_{2.5}$ , the Y coordinate indicating the general decreasing trend in concentrations from south to north, and major roads in the intermediate buffer. As with  $NO_2$ , for  $PM_{10}$  the satellite measurement is consistently the first or second variable to enter the model. Distance to sea enters all but the 2007 model, which instead has the altitude variable. The 2005, 2006, and 2005–2007 models include land cover classes representing both built

up areas and remote areas. The structure of the 2007 model is rather different and includes minor roads in both a local (200 m) and intermediate (200–2500 m) buffer and percent tree canopy as the only land cover variable. Satellite-based  $PM_{2.5}$  and the Y coordinate each contribute  $\sim 30$ – $35\%$  to the model predictive power in each year (see Table S7; partial  $R^2$ : 0.1–0.2).

Based on model  $R^2$ , the year-2007 model explains  $\sim 47\%$  of the variation in measured concentrations ( $\sim 50\%$  of the variation in log-transformed  $NO_2$ ) at the sites reserved for model evaluation; models for earlier years explain 38–44% of variation in measured concentrations (Table S8; Figure S6). Error and bias are relatively similar across years, with lower error and bias in later years: error ( $-0.2$  –  $-1.2$   $\mu g/m^3$ ); absolute error (4.4–6.0  $\mu g/m^3$ ); mean bias (3–5%); absolute bias (17–22%).

#### 4. DISCUSSION

LUR models given here explain 46–56% (36–48%) of the variation in annual mean  $NO_2$  ( $PM_{10}$ ) concentration at independent sites. For both pollutants, satellite data are consistently the first or second variable into the model, and those data improve LUR model performance. Based on model  $R^2$ , satellite data contribute more to the  $PM_{10}$  models than the  $NO_2$  models, despite the difference in particle sizes (using  $PM_{2.5}$  satellite data to model  $PM_{10}$  measurements). This finding is likely because the satellite data provide estimates averaged over a  $\sim 10$  km grid and thus reflects regional background rather than local variations in concentrations. Compared to  $NO_2$ , ambient concentrations of  $PM_{10}$  are much more affected by long-range transport; that transport is detected by the  $PM_{2.5}$  satellite data.

The overall performance of the  $NO_2$  model is better than for  $PM_{10}$ , perhaps owing to other more local predictor variables, consistent with observations in the ESCAPE study.<sup>37,38</sup> Furthermore, in the EU methodological consistency of monitoring is greater for  $NO_2$  (chemiluminescence) than  $PM_{10}$  (multiple methods). Recent spatiotemporal LURs for the USA reported an  $R^2$  of 0.78 for  $NO_2$ <sup>17</sup> and 0.63 for  $PM_{2.5}$ .<sup>16</sup> As indicated by our models with country indicators (Tables S4 and S5) and the evaluation by region (Table S2), however, there are differences between countries which cannot be explained by the variables in our final  $PM_{10}$  models. This perhaps points to the need for regional models, especially for  $PM_{10}$ .

We expect that meteorological conditions also play a role in  $PM_{10}$  model performance. In Europe, for example, 2006 was a year with several air pollution episodes including that associated with the July heat wave. Here, unlike in our previous work,<sup>19,39</sup> we did not specifically include coarse-scale meteorological variables. We took this *a priori* decision because the effects of meteorology are generally captured by the satellite-derived air pollution data, yet at a higher spatial resolution than for meteorological data. While daily meteorological variability is incorporated into the satellite-derived  $PM_{2.5}$  estimates, year-to-year variability, however, is not captured by the long-term mean (2001–2006) we use in the  $PM_{10}$  LUR models. If year-to-year model variation is in fact mainly driven by meteorological factors, model performance may benefit from including meteorological variables in the LUR models or, like  $NO_2$ , using annual satellite data.

In general, the models described here exhibit comparable performance as previous LUR models at the European scale: Beelen et al.<sup>19</sup> report validation  $R^2$ s of 0.61 (0.45) for  $NO_2$  ( $PM_{10}$ ) using a hybrid Kriging-LUR approach. Our  $NO_2$

models may explain less of the variation in measured concentrations relative to the work of Beelen et al. in part because we model all site types, including traffic, rather than only background sites. We found that evaluation  $R^2$ s for independent monitoring sites is very similar to the model  $R^2$ , consistent with methodological work showing that model  $R^2$  can exceed independent evaluation  $R^2$ s for small data sets, but less so for large data sets such as the ones we use here.<sup>40,41</sup>

An important next step for this research would be to model  $PM_{2.5}$ , a pollutant which is subject to recent EU guideline limits<sup>23</sup> and, based on the Global Burden of Disease estimates, is responsible for 3.2 million deaths and 76 million years of lost healthy life worldwide.<sup>42</sup> Although site numbers for  $PM_{2.5}$  are slowly increasing, for this time period and study area, too few sites are available to derive reliable LUR models (146 and 195, respectively, in year-2005 and 2007 with sufficient annual data capture). A large fraction of the spatial variation of  $PM_{10}$  is related to variation of  $PM_{2.5}$ . The ESCAPE study reported an average  $R^2$  between spatial variation of  $PM_{10}$  and  $PM_{2.5}$  of 0.74 (range 0.44–0.95).<sup>30</sup>

Modeling over large areas at fine spatial resolutions is an attractive solution for a variety of applications with large study populations, including health risk assessment. Given that LUR models generally cannot be directly transferred to other spatial domains,<sup>10,11,14</sup> our approach addresses a particular need for reliable and consistent models at the continental level. From our models we estimate the mean population-weighted exposure in 2007 was 27 (25)  $\mu g/m^3$  for  $NO_2$  ( $PM_{10}$ ). Furthermore, we estimate that 9% ( $NO_2$ ) and 1% ( $PM_{10}$ ) of the European population reside in areas exceeding the annual guideline limit of 40  $\mu g/m^3$  (current annual guidelines are the same for  $NO_2$  and  $PM_{10}$ ).<sup>23</sup> Some caution is needed in interpretation of these results given differences in model performance by region (Table S2). These regional differences in model performance may in part be attributable to known deficiencies in the monitoring network (uneven distribution and clustering of sites in EuroAirmet, which is an assembly of sites from existing country networks; use of different  $PM_{10}$  monitoring methods and correction factors by country) or discrepancies in the definition of land cover or road classes across Europe.<sup>43</sup>

There are several challenges in producing suitable models for air pollution exposure assessment across large areas. We aim here for models at a spatial scale fine enough to estimate within-city and near-roadway contrasts in pollution while also accounting for long-range transport and other large scale variability. Most studies evaluating exposures over large areas use a vector-LUR approach whereby estimates are then made at census centroids, a coarse mesh, or home addresses; should a map or estimates at additional locations be required, interpolation is then used to produce a continuous surface.<sup>17,18,44–46</sup> A strength of our models is that we take a raster-based LUR approach, which enables direct prediction at the 100 m grid (Figure 1 and 2). We thus eliminate the need for interpolation which can oversmooth estimates. In this study, a 100 m resolution is justified given the quality and resolution of the source information as well as the dense network of monitoring sites distributed in different exposure environments across Europe. Although not always reflected in the  $R^2$  as a performance measure, this attribute (large number of monitors, located in diverse environments) is an important advance over the previous models for Europe.<sup>19,39</sup>

As was previously demonstrated in Canada<sup>18</sup> and the USA,<sup>16,17,47</sup> we show here that combining LUR models with worldwide, satellite-based pollution measurements can offer improved continental-scale exposure models for Europe. To support future research, model results are publicly available.

## ■ ASSOCIATED CONTENT

### ■ Supporting Information

Table S1: Number of monitoring sites by year. Table S2: Evaluation statistics by regions for best models (based on concentration ( $\mu\text{g}/\text{m}^3$ )). Table S3: Sensitivity analysis - rotating 20% evaluation subsets. Table S4: Sensitivity analysis - NO<sub>2</sub> models based on all monitoring sites. Table S5: Sensitivity analysis - PM<sub>10</sub> models based on all monitoring sites. Table S6: Final NO<sub>2</sub> models by year. Table S7: Final PM<sub>10</sub> models by year. Table S8: Summary of model building and evaluation statistics. Figure S1: Measured ground-based NO<sub>2</sub> vs satellite-derived NO<sub>2</sub> at all monitoring sites. Figure S2: Measured ground-based PM<sub>10</sub> vs mean 2001–2006 satellite-derived PM<sub>2.5</sub> at all monitoring sites. Figure S3: Map and profile plots of NO<sub>2</sub> concentration in 2005 without satellite data; scatterplot of modeled vs measured NO<sub>2</sub> at evaluation sites. Figure S4: Map and profile plots of PM<sub>10</sub> concentration in 2007 without satellite data; scatterplot of modeled vs measured PM<sub>10</sub> at evaluation sites. Figure S5: Modeled vs measured NO<sub>2</sub> concentration ( $\mu\text{g}/\text{m}^3$ ) at evaluation sites for final models. Figure S6: Modeled vs measured PM<sub>10</sub> concentration ( $\mu\text{g}/\text{m}^3$ ) at evaluation sites for final models. This material is available free of charge via the Internet at <http://pubs.acs.org>.

## ■ AUTHOR INFORMATION

### Corresponding Author

\*Phone: +41 (0)61 284 8398. Fax: +41 (0)61 284 8105. E-mail: [danielle.vienneau@unibas.ch](mailto:danielle.vienneau@unibas.ch).

### Notes

The authors declare no competing financial interest.

## ■ ACKNOWLEDGMENTS

The research leading to these results has received funding from the European Community's Seventh Framework Program (FP7/2007-2011) under Grant Agreement No. 211250 and is based upon work supported by the National Science Foundation under Grant No. 0853467. We thank Dr. Eric Novotny for assistance in obtaining and processing the global land use data. We acknowledge the free use of tropospheric NO<sub>2</sub> column data from the OMI sensor via [www.temis.nl](http://www.temis.nl).

## ■ REFERENCES

- Briggs, D. J.; Collins, S.; Elliott, P.; Fischer, P.; Kingham, S.; Lebret, E.; Pryn, K.; van Reeuwijk, H.; Smallbone, K.; van der Veen, A. Mapping urban air pollution using GIS: a regression-based approach. *Int. J. GIS* **1997**, *11* (7), 699–718.
- Jerrett, M.; Arain, A.; Kanaroglou, P.; Beckerman, B.; Potoglou, D.; Sahsuvaroglu, T.; Morrison, J.; Giovis, C. A review and evaluation of intraurban air pollution exposure models. *J. Exposure Sci. Environ. Epidemiol.* **2005**, *15* (2), 185–204.
- Hoek, G.; Beelen, R.; de Hoogh, K.; Vienneau, D.; Gulliver, J.; Fischer, P.; Briggs, D. A review of land-use regression models to assess spatial variation of outdoor air pollution. *Atmos. Environ.* **2008**, *42* (33), 7561–7578.
- Marshall, J. D.; Nethery, E.; Brauer, M. Within-urban variability in ambient air pollution: Comparison of estimation methods. *Atmos. Environ.* **2008**, *42* (6), 1359–1369.

- Gulliver, J.; de Hoogh, K.; Fecht, D.; Vienneau, D.; Briggs, D. Comparative assessment of GIS-based methods and metrics for estimating long-term exposures to air pollution. *Atmos. Environ.* **2011**, *45* (39), 7072–7080.

- de Hoogh, K.; Wang, M.; Adam, M.; Badaloni, C.; Beelen, R.; Birk, M.; Cesaroni, G.; Cirach, M.; Declercq, C.; Dèdelè, A.; Dons, E.; de Nazelle, A.; Eeftens, M.; Eriksen, K. T.; Eriksson, C.; Fischer, P.; Gražulevičienė, R.; Gryparis, A.; Hoffmann, B.; Jerrett, M.; Katsouyanni, K.; Iakovides, M.; Lanki, T.; Lindley, S.; Madsen, C.; Mölter, A.; Mosler, G.; Nádor, G.; Nieuwenhuijsen, M. J.; Pershagen, G.; Peters, A.; Phuleria, H.; Probst-Hensch, N.; Raaschou-Nielsen, O.; Quass, U.; Ranzi, A.; Stephanou, E. G.; Sugiri, D.; Schwarze, P.; Tsai, M.-Y.; Yli-Tuomi, T.; Varró, M. J.; Vienneau, D.; Weinmayr, G.; Brunekreef, B.; Hoek, G. Development of land use regression models for particle composition in 20 study areas in Europe. *Environ. Sci. Technol.* **2013**, *47* (11), 5778–5786.

- Saraswat, A.; Apte, J.; Kandlikar, M.; Brauer, M.; Henderson, S.; Marshall, J. Spatiotemporal land use regression models of fine, ultrafine and black carbon particulate matter in New Delhi, India. *Environ. Sci. Technol.* **2013**, DOI: 10.1021/es401489h.

- Noth, E. M.; Hammond, S. K.; Biging, G. S.; Tager, I. B. A spatial-temporal regression model to predict daily outdoor residential PAH concentrations in an epidemiologic study in Fresno, CA. *Atmos. Environ.* **2011**, *45* (14), 2394–2403.

- Gulliver, J.; de Hoogh, K.; Hansell, A.; Vienneau, D. Development and back-extrapolation of NO<sub>2</sub> land use regression models for historic exposure assessment in Great Britain. *Environ. Sci. Technol.* **2013**, DOI: 10.1021/es4008849.

- Allen, R. W.; Amram, O.; Wheeler, A. J.; Brauer, M. The transferability of NO and NO<sub>2</sub> land use regression models between cities and pollutants. *Atmos. Environ.* **2011**, *45* (2), 369–378.

- Vienneau, D.; de Hoogh, K.; Beelen, R.; Fischer, P.; Hoek, G.; Briggs, D. Comparison of land-use regression models between Great Britain and the Netherlands. *Atmos. Environ.* **2010**, *44* (5), 688–696.

- Poplawski, K.; Gould, T.; Setton, E.; Allen, R.; Su, J.; Larson, T.; Henderson, S.; Brauer, M.; Hystad, P.; Lightowlers, C.; Keller, P.; Cohen, M.; Silva, C.; Buzzelli, M. Intercity transferability of land use regression models for estimating ambient concentrations of nitrogen dioxide. *J. Exposure Sci. Environ. Epidemiol.* **2009**, *19* (1), 107–117.

- Mercer, L. D.; Szpiro, A. A.; Sheppard, L.; Lindström, J.; Adar, S. D.; Allen, R. W.; Avol, E. L.; Oron, A. P.; Larson, T.; Liu, L. J. S.; Kaufman, J. D. Comparing universal kriging and land-use regression for predicting concentrations of gaseous oxides of nitrogen (NO<sub>x</sub>) for the Multi-Ethnic Study of Atherosclerosis and Air Pollution (MESA Air). *Atmos. Environ.* **2011**, *45* (26), 4412–4420.

- Liu, L. J. S.; Tsai, M.-Y.; Keidel, D.; Gemperli, A.; Ineichen, A.; Hazenkamp-von Arx, M.; Bayer-Oglesby, L.; Rochat, T.; Künzli, N.; Ackermann-Liebrich, U.; Straehl, P.; Schwartz, J.; Schindler, C. Long-term exposure models for traffic related NO<sub>2</sub> across geographically diverse areas over separate years. *Atmos. Environ.* **2012**, *46*, 460–471.

- Gulliver, J.; Morris, C.; Lee, K.; Vienneau, D.; Briggs, D.; Hansell, A. Land use regression modeling to estimate historic (1962–1991) concentrations of black smoke and sulfur dioxide for Great Britain. *Environ. Sci. Technol.* **2011**, *45* (8), 3526–3532.

- Beckerman, B. S.; Jerrett, M.; Serre, M.; Martin, R. V.; Lee, S.-J.; van Donkelaar, A.; Ross, Z.; Su, J.; Burnett, R. T. A hybrid approach to estimating national scale spatiotemporal variability of PM<sub>2.5</sub> in the contiguous United States. *Environ. Sci. Technol.* **2013**, *47* (13), 7233–7241.

- Novotny, E. V.; Bechle, M. J.; Millet, D. B.; Marshall, J. D. National satellite-based land-use regression: NO<sub>2</sub> in the United States. *Environ. Sci. Technol.* **2011**, *45* (10), 4407–4414.

- Hystad, P.; Setton, E.; Cervantes, A.; Poplawski, K.; Deschenes, S.; Brauer, M.; van Donkelaar, A.; Lamsal, L.; Martin, R.; Jerrett, M.; Demers, P. Creating national air pollution models for population exposure assessment in Canada. *Environ. Health Perspect.* **2011**, *119* (8), 1123–1129.

- Beelen, R.; Hoek, G.; Pebesma, E.; Vienneau, D.; de Hoogh, K.; Briggs, D. J. Mapping of background air pollution at a fine spatial scale



across the European Union. *Sci. Total Environ.* **2009**, *407* (6), 1852–1867.

(20) Larssen, S.; Sluyter, R.; Helmis, C. *Criteria for EUROAIRNET. The EEA Air Quality Monitoring and Information Network*; European Environment Agency: 1999; pp 2–56.

(21) EEA AirBase - The European air quality database, version 5. <http://www.eea.europa.eu/data-and-maps/data/airbase-the-european-air-quality-database-4> (accessed October 30, 2013).

(22) ETC/ACC Correction factors and PM10 measurements in AirBase; Draft technical paper 2004/x; European Topic Centre on Air and Climate Change, Bilthoven, Netherlands.

(23) Directive 2008/50/EC of the European Parliament and of the Council of 21 May 2008 on ambient air quality and cleaner air for Europe. In *Official Journal of the European Union*: EU, EC 2008; p 44.

(24) van Donkelaar, A.; Martin, R. V.; Brauer, M.; Kahn, R.; Levy, R.; Verduzco, C.; Villeneuve, P. J. Global estimates of ambient fine particulate matter concentrations from satellite-based aerosol optical depth: Development and application. *Environ. Health Perspect.* **2010**, *118* (6), 847–855.

(25) Boersma, K. F.; Eskes, H. J.; Veeffkind, J. P.; Brinksma, E. J.; van der A, R. J.; Sneep, M.; van den Oord, G. H. J.; Levelt, P. F.; Stammes, P.; Gleason, J. F.; Bucsela, E. J. Near-real time retrieval of tropospheric NO<sub>2</sub> from OMI. *Atmos. Chem. Phys.* **2007**, *7* (8), 2103–2118.

(26) Levy, R. C.; Remer, L. A.; Mattoo, S.; Vermote, E. F.; Kaufman, Y. J. Second-generation operational algorithm: Retrieval of aerosol properties over land from inversion of Moderate Resolution Imaging Spectroradiometer spectral reflectance. *J. Geophys. Res.: Atmos.* **2007**, *112*, (D13).

(27) Diner, D. J.; Beckert, J. C.; Reilly, T. H.; Bruegge, C. J.; Conel, J. E.; Kahn, R. A.; Martonchik, J. V.; Ackerman, T. P.; Davies, R.; Gerstl, S. A. W.; Gordon, H. R.; Muller, J.-P.; Myneni, R. B.; Sellers, P. J.; Pinty, B.; Verstraete, M. M. Multi-angle Imaging SpectroRadiometer (MISR) instrument description and experiment overview. *IEEE Trans. Geosci. Remote Sens.* **1998**, *36* (4), 1072–1087.

(28) Bechle, M. J.; Millet, D. B.; Marshall, J. D. Remote sensing of exposure to NO<sub>2</sub>: Satellite versus ground-based measurement in a large urban area. *Atmos. Environ.* **2013**, *69*, 345–353.

(29) EEA Air quality in Europe - 2012 report; No 4/2012; European Environment Agency: Copenhagen, 2012; p 104.

(30) Eeftens, M.; Tsai, M.-Y.; Ampe, C.; Anwander, B.; Beelen, R.; Bellander, T.; Cesaroni, G.; Cirach, M.; Cyrys, J.; de Hoogh, K.; De Nazelle, A.; de Vocht, F.; Declercq, C.; Dèdelè, A.; Eriksen, K.; Galassi, C.; Gražulevičienė, R.; Grivas, G.; Heinrich, J.; Hoffmann, B.; Iakovides, M.; Ineichen, A.; Katsouyanni, K.; Korek, M.; Krämer, U.; Kuhlbusch, T.; Lanki, T.; Madsen, C.; Meliefste, K.; Mölter, A.; Mosler, G.; Nieuwenhuijsen, M.; Oldenwening, M.; Pennanen, A.; Probst-Hensch, N.; Quass, U.; Raaschou-Nielsen, O.; Ranzi, A.; Stephanou, E.; Sugiri, D.; Udvardy, O.; Vaskövi, É.; Weinmayr, G.; Brunekreef, B.; Hoek, G. Spatial variation of PM<sub>2.5</sub>, PM<sub>10</sub>, PM<sub>2.5</sub> absorbance and PMcoarse concentrations between and within 20 European study areas and the relationship with NO<sub>2</sub> – Results of the ESCAPE project. *Atmos. Environ.* **2012**, *62*, 303–317.

(31) ETC-LC Corine land cover (CLC2000), raster database (version 12/2009). <http://www.eea.europa.eu/data-and-maps/data/corine-land-cover-2000-clc2000-100-m-version-12-2009> (accessed October 30, 2013).

(32) Hansen, M.; DeFries, R.; Townshend, J. R.; Carroll, M.; Dimiceli, C.; Sohlberg, R. *Vegetation Continuous Fields MOD44B, 2001 Percent Tree Cover, Collection 4, version 2001*; University of Maryland, College Park, MD, 2006.

(33) Elvidge, C.; Tuttle, B.; Sutton, P.; Baugh, K.; Howard, A.; Milesi, C.; Bhaduri, B.; Nemani, R. Global distribution and density of constructed impervious surfaces. *Sensors* **2007**, *7* (9), 1962–1979.

(34) Gallego, F. J. A population density grid of the European Union. *Popul. Environ.* **2010**, *31* (6), 460–473.

(35) INTARESE EU age/sex stratified population: 100 metre grid. [http://www.integrated-assessment.eu/resource\\_centre/eu\\_agesex\\_stratified\\_population\\_100\\_metre\\_grid](http://www.integrated-assessment.eu/resource_centre/eu_agesex_stratified_population_100_metre_grid) (accessed October 30, 2013).

(36) CGIAR-CSI SRTM 90m Digital Elevation Data. <http://srtm.csi.cgiar.org/> (accessed October 30, 2013).

(37) Eeftens, M.; Beelen, R.; de Hoogh, K.; Bellander, T.; Cesaroni, G.; Cirach, M.; Declercq, C.; Dèdelè, A.; Dons, E.; de Nazelle, A.; Dimakopoulou, K.; Eriksen, K.; Falq, G.; Fischer, P.; Galassi, C.; Gražulevičienė, R.; Heinrich, J.; Hoffmann, B.; Jerrett, M.; Keidel, D.; Korek, M.; Lanki, T.; Lindley, S.; Madsen, C.; Mölter, A.; Nádor, G.; Nieuwenhuijsen, M.; Nonnemacher, M.; Pedeli, X.; Raaschou-Nielsen, O.; Patelarou, E.; Quass, U.; Ranzi, A.; Schindler, C.; Stempfelet, M.; Stephanou, E.; Sugiri, D.; Tsai, M.-Y.; Yli-Tuomi, T.; Varró, M. J.; Vienneau, D.; Klot, S. v.; Wolf, K.; Brunekreef, B.; Hoek, G. Development of land use regression models for PM<sub>2.5</sub>, PM<sub>2.5</sub> absorbance, PM<sub>10</sub> and PMcoarse in 20 European study areas; Results of the ESCAPE Project. *Environ. Sci. Technol.* **2012**, *46* (20), 11195–11205.

(38) Beelen, R.; Hoek, G.; Vienneau, D.; Eeftens, M.; Dimakopoulou, K.; Pedeli, X.; Tsai, M.-Y.; Künzli, N.; Schikowski, T.; Marcon, A.; Eriksen, K. T.; Raaschou-Nielsen, O.; Stephanou, E.; Patelarou, E.; Lanki, T.; Yli-Tuomi, T.; Declercq, C.; Falq, G.; Stempfelet, M.; Birk, M.; Cyrys, J.; von Klot, S.; Nádor, G.; Varró, M. J.; Dèdelè, A.; Gražulevičienė, R.; Mölter, A.; Lindley, S.; Madsen, C.; Cesaroni, G.; Ranzi, A.; Badaloni, C.; Hoffmann, B.; Nonnemacher, M.; Krämer, U.; Kuhlbusch, T.; Cirach, M.; de Nazelle, A.; Nieuwenhuijsen, M.; Bellander, T.; Korek, M.; Olsson, D.; Strömberg, M.; Dons, E.; Jerrett, M.; Fischer, P.; Wang, M.; Brunekreef, B.; de Hoogh, K. Development of NO<sub>2</sub> and NO<sub>x</sub> land use regression models for estimating air pollution exposure in 36 study areas in Europe – The ESCAPE project. *Atmos. Environ.* **2013**, *72*, 10–23.

(39) Vienneau, D.; de Hoogh, K.; Briggs, D. A GIS-based method for modelling air pollution exposures across Europe. *Sci. Total Environ.* **2009**, *408* (2), 255–266.

(40) Wang, M.; Beelen, R.; Eeftens, M.; Meliefste, K.; Hoek, G.; Brunekreef, B. Systematic evaluation of land use regression models for NO<sub>2</sub>. *Environ. Sci. Technol.* **2012**, *46* (8), 4481–4489.

(41) Basagaña, X.; Rivera, M.; Aguilera, I.; Agis, D.; Bouso, L.; Elosua, R.; Foraster, M.; de Nazelle, A.; Nieuwenhuijsen, M.; Vila, J.; Künzli, N. Effect of the number of measurement sites on land use regression models in estimating local air pollution. *Atmos. Environ.* **2012**, *54*, 634–642.

(42) Lim, S. S.; Vos, T.; Flaxman, A. D.; Danaei, G.; Shibuya, K.; Adair-Rohani, H.; Amann, M.; Anderson, H. R.; Andrews, K. G.; Aryee, M.; Atkinson, C.; Bacchus, L. J.; Bahalim, A. N.; Balakrishnan, K.; Balmes, J.; Barker-Collo, S.; Baxter, A.; Bell, M. L.; Blore, J. D.; Blyth, F.; Bonner, C.; Borges, G.; Bourne, R.; Boussinesq, M.; Brauer, M.; Brooks, P.; Bruce, N. G.; Brunekreef, B.; Bryan-Hancock, C.; Bucello, C.; Buchbinder, R.; Bull, F.; Burnett, R. T.; Byers, T. E.; Calabria, B.; Carapetis, J.; Carnahan, E.; Chafe, Z.; Charlson, F.; Chen, H.; Chen, J. S.; Cheng, A. T.; Child, J. C.; Cohen, A.; Colson, K. E.; Cowie, B. C.; Darby, S.; Darling, S.; Davis, A.; Degenhardt, L.; Dentener, F.; Des Jarlais, D. C.; Devries, K.; Dherani, M.; Ding, E. L.; Dorsey, E. R.; Driscoll, T.; Edmond, K.; Ali, S. E.; Engell, R. E.; Erwin, P. J.; Fahimi, S.; Falder, G.; Farzadfar, F.; Ferrari, A.; Finucane, M. M.; Flaxman, S.; Fowkes, F. G.; Freedman, G.; Freeman, M. K.; Gakidou, E.; Ghosh, S.; Giovannucci, E.; Gmel, G.; Graham, K.; Grainger, R.; Grant, B.; Gunnell, D.; Gutierrez, H. R.; Hall, W.; Hoek, H. W.; Hogan, A.; Hosgood, H. D., 3rd; Hoy, D.; Hu, H.; Hubbard, B. J.; Hutchings, S. J.; Ibeanusi, S. E.; Jacklyn, G. L.; Jasrasaria, R.; Jonas, J. B.; Kan, H.; Kanis, J. A.; Kassebaum, N.; Kawakami, N.; Khang, Y. H.; Khatibzadeh, S.; Khoo, J. P.; Kok, C.; Laden, F.; Lalloo, R.; Lan, Q.; Lathlean, T.; Leasher, J. L.; Leigh, J.; Li, Y.; Lin, J. K.; Lipshultz, S. E.; London, S.; Lozano, R.; Lu, Y.; Mak, J.; Malekzadeh, R.; Mallinger, L.; Marcenes, W.; March, L.; Marks, R.; Martin, R.; McGale, P.; McGrath, J.; Mehta, S.; Mensah, G. A.; Merriman, T. R.; Micha, R.; Michaud, C.; Mishra, V.; Hanafiah, K. M.; Mokdad, A. A.; Morawska, L.; Mozaffarian, D.; Murphy, T.; Naghavi, M.; Neal, B.; Nelson, P. K.; Nolla, J. M.; Norman, R.; Olives, C.; Omer, S. B.; Orchard, J.; Osborne, R.; Ostro, B.; Page, A.; Pandey, K. D.; Parry, C. D.; Passmore, E.; Patra, J.; Pearce, N.; Pelizzari, P. M.; Petzold, M.; Phillips, M. R.; Pope, D.; Pope, C. A., 3rd; Powles, J.; Rao, M.; Razavi,

H.; Rehfuess, E. A.; Rehm, J. T.; Ritz, B.; Rivara, F. P.; Roberts, T.; Robinson, C.; Rodriguez-Portales, J. A.; Romieu, I.; Room, R.; Rosenfeld, L. C.; Roy, A.; Rushton, L.; Salomon, J. A.; Sampson, U.; Sanchez-Riera, L.; Sanman, E.; Sapkota, A.; Seedat, S.; Shi, P.; Shield, K.; Shivakoti, R.; Singh, G. M.; Sleet, D. A.; Smith, E.; Smith, K. R.; Stapelberg, N. J.; Steenland, K.; Stockl, H.; Stovner, L. J.; Straif, K.; Straney, L.; Thurston, G. D.; Tran, J. H.; Van Dingenen, R.; van Donkelaar, A.; Veerman, J. L.; Vijayakumar, L.; Weintraub, R.; Weissman, M. M.; White, R. A.; Whiteford, H.; Wiersma, S. T.; Wilkinson, J. D.; Williams, H. C.; Williams, W.; Wilson, N.; Woolf, A. D.; Yip, P.; Zielinski, J. M.; Lopez, A. D.; Murray, C. J.; Ezzati, M.; AlMazroa, M. A.; Memish, Z. A. A comparative risk assessment of burden of disease and injury attributable to 67 risk factors and risk factor clusters in 21 regions, 1990–2010: a systematic analysis for the Global Burden of Disease Study 2010. *Lancet* **2012**, *380* (9859), 2224–60.

(43) Vienneau, D.; Briggs, D. J. Delimiting affinity zones as a basis for air pollution mapping in Europe. *Environ. Int.* **2013**, *51*, 106–115.

(44) Hystad, P.; Demers, P.; Johnson, K.; Brook, J.; van Donkelaar, A.; Lamsal, L.; Martin, R.; Brauer, M. Spatiotemporal air pollution exposure assessment for a Canadian population-based lung cancer case-control study. *Environ. Health* **2012**, *11* (1), 22.

(45) Ross, Z.; Jerrett, M.; Ito, K.; Tempalski, B.; Thurston, G. D. A land use regression for predicting fine particulate matter concentrations in the New York City region. *Atmos. Environ.* **2007**, *41* (11), 2255–2269.

(46) Hart, J. E.; Yanosky, J. D.; Puett, R. C.; Ryan, L.; Dockery, D. W.; Smith, T. J.; Garshick, E.; Laden, F. Spatial modeling of PM<sub>10</sub> and NO<sub>2</sub> in the continental United States, 1985–2000. *Environ. Health Perspect.* **2009**, *117* (11), 1690–6.

(47) Kloog, I.; Nordio, F.; Coull, B. A.; Schwartz, J. Incorporating local land use regression and satellite aerosol optical depth in a hybrid model of spatiotemporal PM<sub>2.5</sub> exposures in the Mid-Atlantic States. *Environ. Sci. Technol.* **2012**, *46* (21), 11913–11921.

## Supporting Information

Western European land use regression incorporating satellite- and ground-based measurements of NO<sub>2</sub> and PM<sub>10</sub>

Danielle Vienneau<sup>1,2,3\*</sup>, Kees de Hoogh<sup>3</sup>, Matthew J. Bechle<sup>4</sup>, Rob Beelen<sup>5</sup>, Aaron van Donkelaar<sup>6</sup>, Randall V. Martin<sup>6,7</sup>, Dylan B. Millet<sup>4</sup>, Gerard Hoek<sup>5</sup>, Julian D. Marshall<sup>4</sup>

1. Swiss Tropical and Public Health Institute, Basel, Switzerland
2. University of Basel, Basel, Switzerland
3. MRC-PHE Centre for Environment and Health, Department of Epidemiology and Biostatistics, Imperial College London, United Kingdom
4. Department of Civil Engineering, University of Minnesota, Minneapolis, USA
5. Institute for Risk Assessment Sciences, Division Environmental Epidemiology, Utrecht University, Utrecht, the Netherlands
6. Department of Physics and Atmospheric Science, Dalhousie University, Halifax, Canada
7. Harvard-Smithsonian Center for Astrophysics, Cambridge, Massachusetts, USA

### Contents:

Table S1. Number of monitoring sites by year .....	2
Table S2. Evaluation statistics by regions for best models (based on concentration (µg/m <sup>3</sup> )) .....	3
Table S3. Sensitivity analysis - rotating 20% evaluation subsets .....	4
Table S4. Sensitivity analysis - NO <sub>2</sub> models based on all monitoring sites.....	5
Table S5. Sensitivity analysis - PM <sub>10</sub> models based on all monitoring sites .....	6
Table S6. Final NO <sub>2</sub> models by year.....	7
Table S7. Final PM <sub>10</sub> models by year .....	8
Table S8. Summary of model building and evaluation statistics .....	9
Figure S1. Measured ground-based NO <sub>2</sub> vs. satellite-derived NO <sub>2</sub> , at all monitoring sites.....	10
Figure S2. Measured ground-based PM <sub>10</sub> vs. mean 2001-2006 satellite-derived PM <sub>2.5</sub> , at all monitoring sites.....	11
Figure S3. Map and profile plots of NO <sub>2</sub> concentration in 2005 without satellite data; scatterplot of modelled vs. measured NO <sub>2</sub> at evaluation sites .....	12
Figure S4. Map and profile plots of PM <sub>10</sub> concentration in 2007 without satellite data; scatterplot of modelled vs. measured PM <sub>10</sub> at evaluation sites.....	13
Figure S5. Modelled vs. measured NO <sub>2</sub> concentration (µg/m <sup>3</sup> ) at evaluation sites for final models shown in Tables S3 and S5 .....	14
Figure S6. Modelled vs. measured PM <sub>10</sub> concentration (µg/m <sup>3</sup> ) at evaluation sites for final models shown in Tables S4 and S5.....	15

**Table S1. Number of monitoring sites by year**

Country	NO <sub>2</sub> Sites				PM <sub>10</sub> Sites			
	2005	2006	2007	2005-2007	2005	2006	2007	2005-2007
AT	146	145	151	138	107	109	127	98
BE	56	57	62	48	39	39	44	35
DE	394	409	419	358	371	400	417	329
DK	12	12	12	12	10	6	7	4
ES	352	321	372	261	260	236	241	171
FI	26	29	25	20	31	29	27	20
FR	456	463	456	399	305	299	289	211
GB	92	97	38	31	64	67	47	39
GR	16	20	23	15	6	7	13	4
HU	23	23	21	21	19	23	23	18
IE	6	8	7	4	8	8	11	5
IT	309	379	509	259	159	248	296	127
LT	8	12	12	6	12	12	13	10
LU	5	5	6	4	1	1	3	0
NL	42	50	51	37	36	38	36	33
PT	56	55	56	48	45	42	45	37
SE	11	14	16	9	14	20	25	10
<b>Total</b>	2010	2099	2236	1670	1487	1584	1664	1151

Countries: Austria (AT), Belgium (BE), Denmark (DK), Finland (FI), France (FR), Germany (DE), Greece (GR), Hungary (HU), Ireland (IE), Italy (IT) Lithuania (LT), Luxembourg (LU), the Netherlands (NL), Portugal (PT), Spain (ES), Sweden (SE), United Kingdom (GB)

**Table S2. Evaluation statistics by regions for best models (based on concentration ( $\mu\text{g}/\text{m}^3$ ))**A. Final  $\text{NO}_2$  model, year 2005 (Corine + satellite vs. Corine only)

Regions <sup>a</sup>	At Evaluation Sites <sup>b</sup>					At All Sites				
	With Satellite		Without Satellite		N	With Satellite		Without Satellite		N
	R <sup>2</sup>	RMSE	R <sup>2</sup>	RMSE		R <sup>2</sup>	RMSE	R <sup>2</sup>	RMSE	
Overall	0.56	11.54	0.54	11.82	398	0.51	11.80	0.49	12.04	2010
DK-FI-SE-LT	0.73	8.63	0.75	8.47	11	0.62	8.28	0.58	9.51	57
BE-LU-NL	0.66	7.50	0.67	7.82	25	0.53	10.08	0.54	9.16	103
GB-IE	0.44	16.41	0.40	16.86	19	0.64	12.05	0.61	12.15	98
DE	0.60	8.55	0.61	8.68	69	0.58	9.79	0.65	8.99	394
FR	0.58	9.58	0.59	9.88	90	0.50	10.15	0.48	11.07	456
HU-AT	0.61	9.42	0.60	9.04	26	0.43	11.70	0.46	11.13	169
PT-ES	0.63	9.71	0.61	9.95	93	0.67	10.25	0.64	10.65	408
IT-GR	0.52	17.67	0.50	18.22	65	0.43	17.57	0.41	18.25	325

B. Final  $\text{PM}_{10}$  model, year 2007 (Global + satellite vs. Global only)

Regions <sup>a</sup>	At Evaluation Sites <sup>b</sup>					At All Sites				
	With Satellite		Without Satellite		N	With Satellite		Without Satellite		N
	R <sup>2</sup>	RMSE	R <sup>2</sup>	RMSE		R <sup>2</sup>	RMSE	R <sup>2</sup>	RMSE	
Overall	0.47	6.74	0.37	7.40	325	0.49	6.26	0.35	7.07	1664
DK-FI-SE-LT	0.30	7.29	0.31	5.73	15	0.38	6.64	0.44	5.49	72
BE-LU-NL	0.38	3.38	0.48	3.64	16	0.32	4.28	0.34	4.32	83
GB-IE	0.00	5.20	0.03	5.97	10	0.57	4.40	0.53	5.25	58
DE	0.58	4.03	0.54	4.10	76	0.50	4.12	0.48	4.18	417
FR	0.32	5.54	0.26	5.82	55	0.23	5.27	0.16	5.66	289
HU-AT	0.06	5.16	0.10	5.04	27	0.26	4.94	0.35	4.97	150
PT-ES	0.39	9.67	0.33	9.93	66	0.32	8.52	0.29	8.43	286
IT-GR	0.54	7.86	0.19	10.35	60	0.45	8.02	0.07	11.00	309

a. Regions listed north to south

b. Evaluation sites refers to the 20% sites not used in model building

Countries: Austria (AT), Belgium (BE), Denmark (DK), Finland (FI), France (FR), Germany (DE), Greece (GR), Hungary (HU), Ireland (IE), Italy (IT) Lithuania (LT), Luxembourg (LU), the Netherlands (NL), Portugal (PT), Spain (ES), Sweden (SE), United Kingdom (GB)

**Table S3. Sensitivity analysis - rotating 20% evaluation subsets**

Year	Model	Subset <sup>b</sup>	Model Building <sup>a</sup>	Model Evaluation <sup>b</sup>		Decision
				LN Concentration	Concentration (µg/m <sup>3</sup> )	
			Adj-R <sup>2</sup>	R <sup>2</sup>	R <sup>2</sup>	
<b>NO<sub>2</sub></b>						
2005	Corine with satellite	1	0.58	0.58	0.56	final model
		2	0.58	0.58	0.39	
		3	0.59	0.53	0.45	
		4	0.58	0.60	0.54	
		5	0.58	0.60	0.52	
2006	Corine with satellite	1	0.56	0.52	0.41	reject: spatial autocorrelation
		2	0.55	0.55	0.50	final model
		3	0.56	0.52	0.42	
		4	0.55	0.54	0.47	
		5	0.54	0.60	0.50	
2007	Corine with satellite	1	0.55	0.59	0.50	final model
		2	0.56	0.56	0.41	
		3	0.57	0.50	0.43	
		4	0.56	0.54	0.43	
		5	0.55	0.58	0.52	
<b>PM<sub>10</sub></b>						
2005	Global with satellite	1	0.35	0.41	0.44	final model
		2	0.36	0.34	0.36	
		3	0.36	0.37	0.38	
		4	0.36	0.33	0.35	
		5	0.36	0.29	0.30	
2006	Corine with satellite	1	0.35	0.40	0.38	reject: spatial autocorrelation
		2	0.36	0.32	0.34	final model
		3	0.38	0.30	0.30	
		4	0.34	0.44	0.43	
		5	0.38	0.29	0.32	
2007	Global with satellite	1	0.50	0.50	0.47	final model
		2	0.50	0.53	0.48	
		3	0.50	0.53	0.52	
		4	0.50	0.53	0.52	
		5	0.53	0.41	0.41	

a. Model building based on natural logarithm of concentration (LN concentration) using 80% of monitoring sites

b. Model evaluation using 20% reserved monitoring sites

**Table S4. Sensitivity analysis - NO<sub>2</sub> models based on all monitoring sites**

Variables	Model building <sup>a</sup>				
	$\beta^b$	IQR	$\beta^* \text{ IQR}$	VIF	Partial Adj-R <sup>2</sup>
2005 - Corine with satellite					
Constant	2.245				
Minor roads 1500m	4.37E-06	56158	0.25	2.6	0.37
Satellite-derived surface NO <sub>2</sub> 2005	6.46E-02	3.0	0.19	1.3	0.49
Major roads 100m	6.02E-04	0.0	0.00	1.1	0.53
Total built up land 300m	3.31E-03	55.2	0.18	2.2	0.56
Minor roads 1500-10000m	1.19E-07	981014	0.12	1.9	0.57
Semi-natural land 600m	-4.03E-03	4.4	-0.02	1.6	0.58
2006 - Corine with satellite					
Constant	2.35				
Minor roads 2000m	2.49E-06	88596	0.22	2.7	0.34
Satellite-derived surface NO <sub>2</sub> 2006	4.30E-02	3.8	0.17	1.2	0.44
Semi-natural land 500m	-4.85E-03	1.2	-0.01	1.6	0.48
Major roads 100m	6.55E-04	0.0	0.00	1.1	0.53
Total built up land 400m	3.44E-03	53.1	0.18	2.2	0.54
Minor roads 2000-10000m	1.07E-07	939846	0.10	1.9	0.55
2007 - Corine with satellite					
Constant	2.28				
Minor roads 1500m	4.35E-06	55676	0.24	2.5	0.33
Satellite-derived surface NO <sub>2</sub> 2007	6.51E-02	3.02	0.20	1.3	0.46
Major roads 100m	6.21E-04	0.00	0.00	1.0	0.50
Semi-natural land 600m	-4.35E-03	4.42	-0.02	1.6	0.53
Total built up land 300m	3.20E-03	55.17	0.18	2.2	0.55
Minor roads 1500-10000m	1.02E-07	917706.00	0.09	1.8	0.56

a. Model building based on natural logarithm of concentration (LN concentration) using 100% of monitoring sites

b. All p-values < 0.000

Adj-R<sup>2</sup> including country dummy variables: 0.62 (year-2005), 0.61 (year-2006) and 0.62 (year-2007)

**Table S5. Sensitivity analysis - PM<sub>10</sub> models based on all monitoring sites**

Variables	Model building <sup>a</sup>			VIF	Partial Adj-R <sup>2</sup>
	$\beta^b$	IQR	$\beta^* \text{ IQR}$		
2005 - Global with satellite					
Constant	3.36				
Tree canopy 500m	-3.45E-03	7.5	-0.03	1.2	.12
Satellite-derived surface PM <sub>2.5</sub> 2001-6	2.10E-02	7.1	0.15	1.1	.20
Y coordinate	-1.93E-07	775844	-0.15	1.1	.30
Impervious surface 800m	2.71E-03	40.5	0.11	1.2	.34
2006 - Corine with satellite					
Constant	3.47				
Satellite-derived surface PM <sub>2.5</sub> 2001-6	2.23E-02	6.9	0.15	1.1	.13
Y coordinate	-1.82E-07	778267	-0.14	1.2	.25
Semi-natural land 1000m	-3.04E-03	10.4	-0.03	1.2	.31
High density residential 1500m	3.04E-03	13.1	0.04	1.2	.34
Major roads 100m	2.05E-04	0.0	0.00	1.1	.35
Distance to sea	-1.87E-01	0.4	-0.07	1.2	.36
2007 - Global with satellite					
Constant	3.65				
Y coordinate	-2.85E-07	780423	-0.22	1.2	.14
Satellite-derived surface PM <sub>2.5</sub> 2001-6	2.00E-02	7.1	0.14	1.1	.30
Impervious surface 1000m	2.32E-03	36.4	0.08	1.4	.42
Altitude	-7.37E-01	0.2	-0.12	1.2	.47
Minor roads 200m	4.59E-05	1564	0.07	1.4	.49
Major roads	4.94E-04	0.0	0.00	1.1	.50

a. Model building based on natural logarithm of concentration (LN concentration) using 100% of monitoring sites

b. All p-values < 0.000

Adj-R<sup>2</sup> including country dummy variables: 0.54 (year-2005), 0.53 (year-2006) and 0.54 (year-2007)



**Table S6. Final NO<sub>2</sub> models by year**

Variables	Model building <sup>a</sup>				
	$\beta^b$	IQR	$\beta^* \text{ IQR}$	VIF	Partial Adj-R <sup>2</sup>
2005 - Corine with satellite					
Constant	2.31				
Minor roads 1800m	3.22E-06	74727	0.24	2.6	0.38
Satellite-derived surface NO <sub>2</sub> 2005	6.13E-02	3.0	0.18	1.3	0.48
Semi-natural land 600m	-4.84E-03	4.4	-0.02	1.6	0.52
Major roads 100m	5.91E-04	0.0	0.00	1.1	0.56
Total built up land 300m	3.15E-03	55.2	0.17	2.1	0.57
Minor roads 1800-10000m	1.04E-07	978059	0.10	2.0	0.58
2006 - Corine with satellite					
Constant	2.35				
Minor roads 1500m	3.96E-06	54683	0.22	2.5	0.33
Satellite-derived surface NO <sub>2</sub> 2006	4.30E-02	4.0	0.17	1.3	0.43
Major roads 100m	6.49E-04	0.0	0.00	1.1	0.48
Semi-natural land 500m	-5.19E-03	1.2	-0.01	1.6	0.52
Minor roads 1500-10000m	1.22E-07	965644	0.12	1.7	0.54
Total built up land 300m	3.10E-03	51.7	0.16	2.2	0.55
2007 - Corine with satellite					
Constant	2.3				
Minor roads 1500m	4.21E-06	55549	0.23	2.6	0.32
Satellite-derived surface NO <sub>2</sub> 2007	6.37E-02	3.1	0.20	1.3	0.45
Major roads 100m	6.33E-04	0.0	0.00	1.0	0.49
Semi-natural land 600m	-4.30E-03	5.3	-0.02	1.6	0.53
Total built up land 300m	3.13E-03	58.6	0.18	2.2	0.54
Minor roads 1500-10000m	1.01E-07	912789	0.09	1.8	0.55
2005-2007 - Corine with satellite					
Constant	2.3				
Minor roads 1500m	4.09E-06	54754	0.22	2.5	0.37
Satellite-derived surface NO <sub>2</sub> 2005-2007 <sup>c</sup>	5.29E-02	3.2	0.17	1.3	0.48
Semi-natural land 600m	-4.79E-03	4.4	-0.02	1.6	0.53
Major roads 100m	5.93E-04	0.0	0.00	1.1	0.57
Minor roads 1500-10000m	1.22E-07	961813	0.12	1.8	0.58
Total built up land 300m	3.16E-03	48.3	0.15	2.3	0.60

a. Model building based on natural logarithm of concentration (LN concentration) using 80% of monitoring sites

b. All p-values < 0.000

c. Average of annual satellite-derived surface NO<sub>2</sub> for the three year period

**Table S7. Final PM<sub>10</sub> models by year**

Variables	Model building <sup>a</sup>				
	$\beta^b$	IQR	$\beta^* \text{ IQR}$	VIF	Partial Adj-R <sup>2</sup>
2005 - Global with satellite					
Constant	3.42				
Y coordinate	-1.87E-07	756842	-0.14	1.1	0.13
Satellite-derived surface PM <sub>2.5</sub> 2001-6	2.26E-02	6.9	0.16	1.1	0.24
Impervious surface 1000m	2.46E-03	39.1	0.10	1.2	0.31
Tree canopy 500m	-2.86E-03	7.7	-0.02	1.3	0.33
Distance to sea	-2.20E-01	0.4	-0.08	1.1	0.34
Major roads	4.47E-04	0.0	0.00	1.1	0.35
2006 - Corine with satellite					
Constant	3.471				
Satellite-derived surface PM <sub>2.5</sub> 2001-6	2.19E-02	6.9	0.15	1.1	0.13
Y coordinate	-2.00E-07	780076	-0.16	1.1	0.26
Total built up land 600m	8.86E-04	52.2	0.05	1.9	0.31
Population 1800m	1.04E-06	38155	0.04	1.3	0.33
Distance to sea	-2.42E-01	0.4	-0.09	1.1	0.35
Major roads 100m	1.97E-04	0.0	0.00	1.1	0.36
Semi-natural land 1000m	-1.77E-03	1.8	0.00	1.6	0.37
2007 - Global with satellite					
Constant	3.67				
Satellite-derived surface PM <sub>2.5</sub> 2001-6	1.93E-02	7.1	0.14	1.1	0.16
Y coordinate	-2.83E-07	778777	-0.22	1.2	0.31
Minor roads 200-2500m	6.03E-07	119820	0.07	1.7	0.42
Altitude	-6.93E-01	0.2	-0.11	1.2	0.47
Minor roads 200m	3.52E-05	1538.0	0.05	1.6	0.48
Major roads	5.07E-04	0.0	0.00	1.1	0.49
Tree canopy 100m	-1.86E-03	8.2	-0.02	1.3	0.50
2005-2007 - Corine with satellite					
Constant	3.61				
Y coordinate	-2.40E-07	683381	-0.16	1.1	0.17
Satellite-derived surface PM <sub>2.5</sub> 2001-6	2.24E-02	7.1	0.16	1.1	0.31
Semi-natural land 1200m	-2.30E-03	12.9	-0.03	1.7	0.40
Distance to sea	-3.45E-01	0.3	-0.11	1.1	0.43
Population 1800m	7.48E-07	37142	0.03	1.3	0.46
Total built up 400m	1.18E-03	51.0	0.06	1.7	0.47
Major roads 100m	1.42E-04	0.0	0.00	1.1	0.48

a. Model building based on natural logarithm of concentration (LN concentration) using 80% of monitoring sites

b. All p-values < 0.000

**Table S8. Summary of model building and evaluation statistics**

Year	Model	Model building <sup>a</sup>			Model Evaluation <sup>b</sup>									N
		Adj-R <sup>2</sup>	SEE	N	LN concentration		Concentration (µg/m <sup>3</sup> )							
					R <sup>2</sup>	SEE	R <sup>2</sup>	RMSE	ME	MAE	MB	MAB	Regression line <sup>c</sup>	
NO <sub>2</sub>														
2005	Corine with satellite	0.58	0.42	1612	0.58	0.44	0.56	11.54	-1.8	8.1	13	37	y=0.98x+2.47	398
2006	Corine with satellite	0.55	0.43	1674	0.55	0.42	0.50	11.35	-1.5	8.3	11	35	y=0.90x+4.15	425
2007	Corine with satellite	0.55	0.42	1786	0.59	0.42	0.50	11.80	-1.3	8.5	18	41	y=0.91x+3.76	450
2005-2007	Corine with satellite	0.60	0.39	1330	0.56	0.42	0.46	11.66	-1.8	8.4	8	34	y=0.84x+6.07	340
PM <sub>10</sub>														
2005	Global with satellite	0.35	0.27	1184	0.41	0.26	0.44	7.07	-0.8	5.4	4	21	y=1.13x-2.53	303
2006	Corine with satellite	0.37	0.26	1263	0.35	0.27	0.36	7.56	-1.2	6.0	3	22	y=1.04x+0.22	321
2007	Global with satellite	0.50	0.23	1339	0.50	0.23	0.47	6.74	-0.5	4.6	4	17	y=1.07x-1.36	325
2005-2007	Corine with satellite	0.48	0.22	895	0.46	0.21	0.48	5.99	-0.2	4.4	3	17	y=1.00x+0.39	256

a. Model building based on natural logarithm of concentration (LN concentration) using 80% of monitoring sites

b. Model evaluation using 20% reserved monitoring sites

c. See Figures S5 and S5 for scatterplots

ME = mean error (µg/m<sup>3</sup>); MAE = mean absolute error (µg/m<sup>3</sup>); MB = mean bias (%); MAB = mean absolute bias (%)

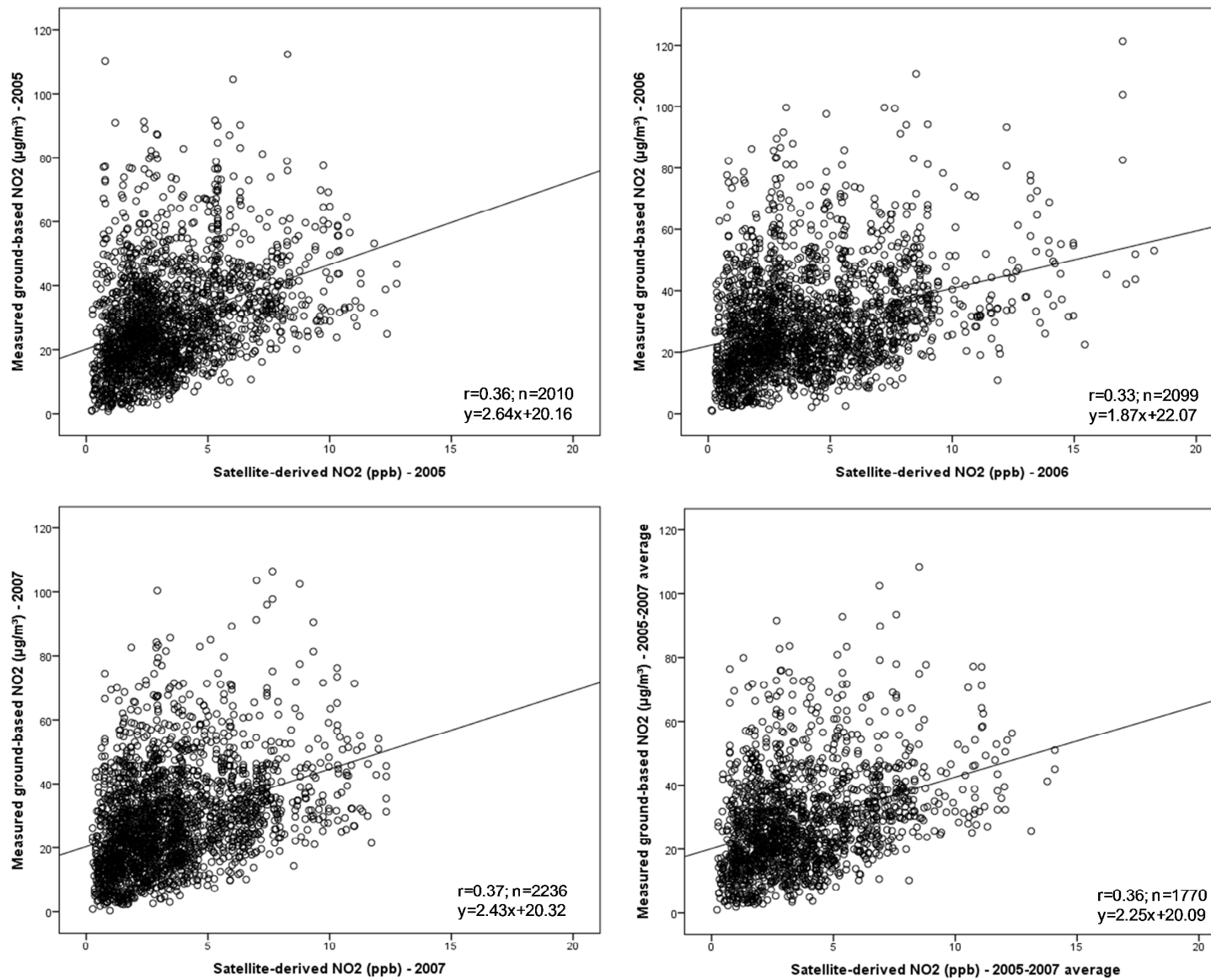


Figure S1. Measured ground-based NO<sub>2</sub> vs. satellite-derived NO<sub>2</sub>, at all monitoring sites

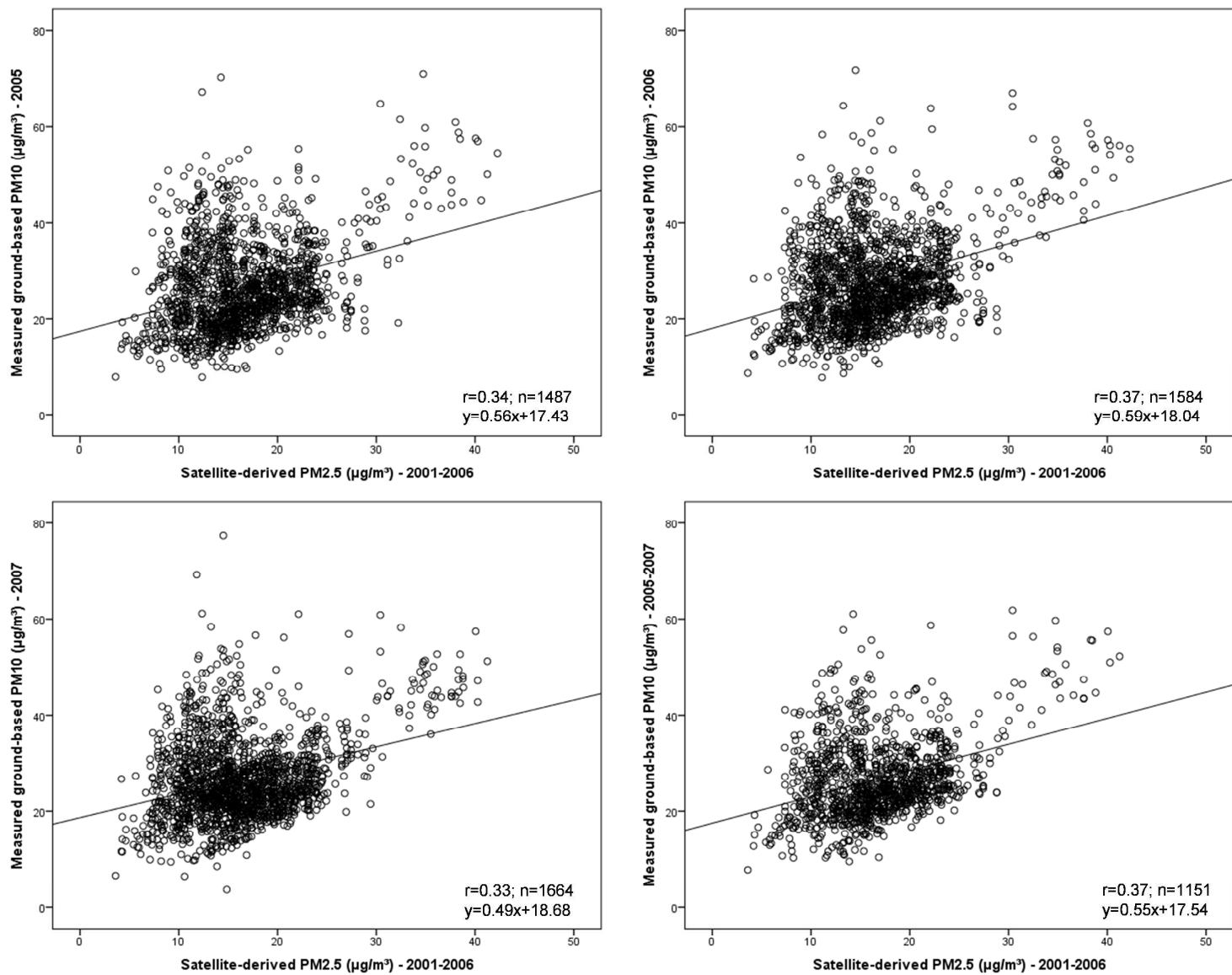


Figure S2. Measured ground-based PM<sub>10</sub> vs. mean 2001-2006 satellite-derived PM<sub>2.5</sub>, at all monitoring sites

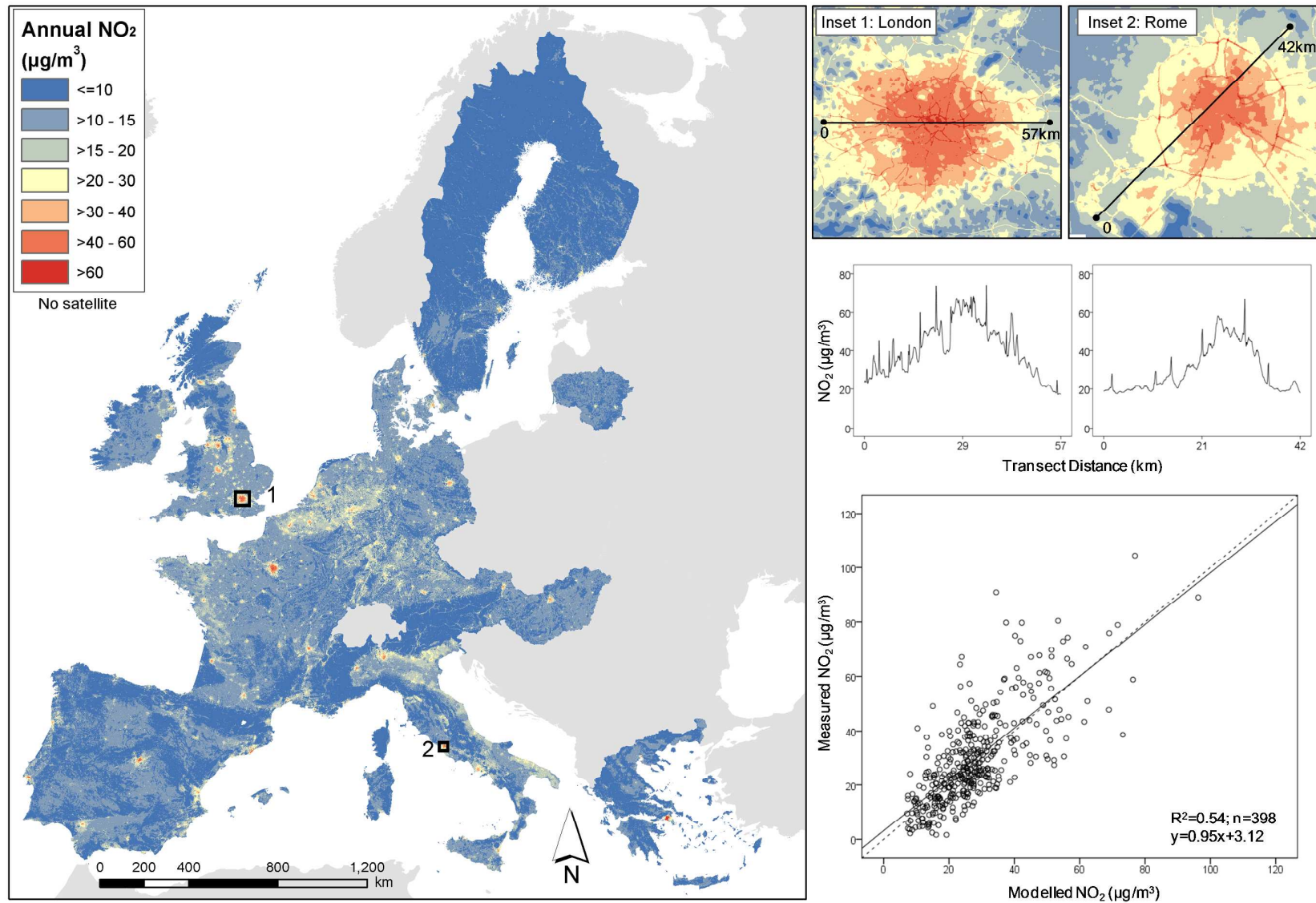


Figure S3. Map and profile plots of NO<sub>2</sub> concentration in 2005 without satellite data; scatterplot of modelled vs. measured NO<sub>2</sub> at evaluation sites

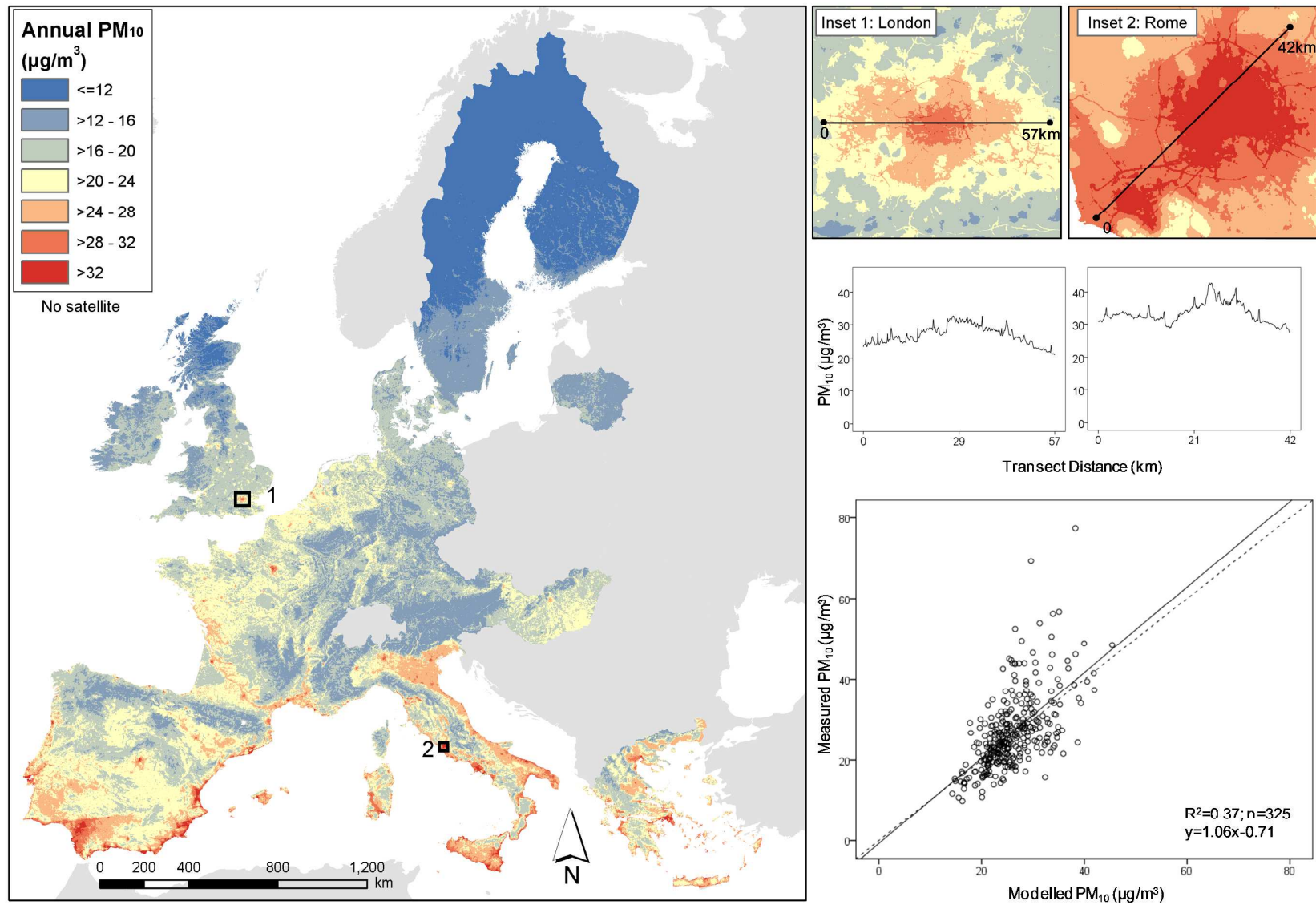


Figure S4. Map and profile plots of PM<sub>10</sub> concentration in 2007 without satellite data; scatterplot of modelled vs. measured PM<sub>10</sub> at evaluation sites

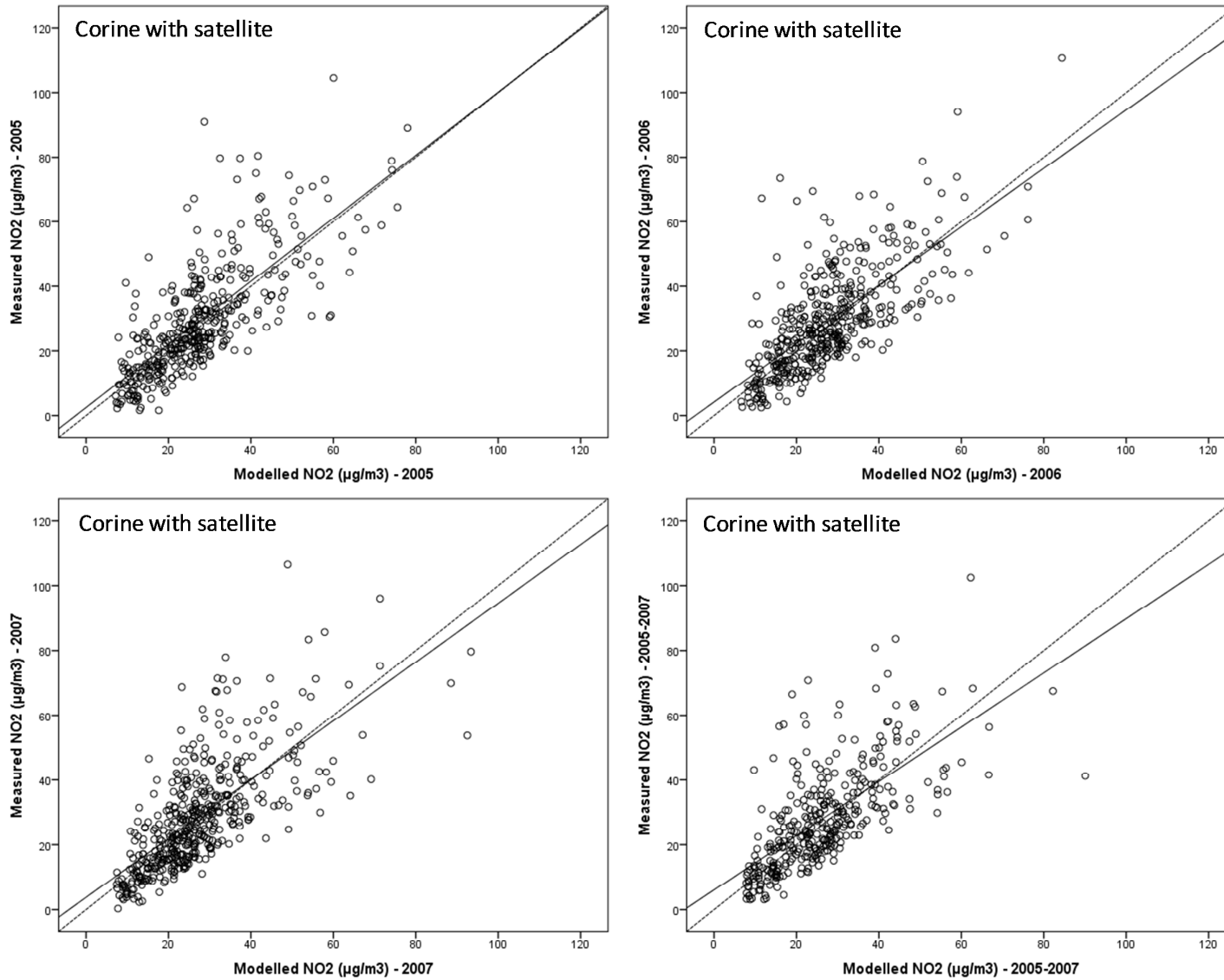


Figure S5. Modelled vs. measured NO<sub>2</sub> concentration (µg/m<sup>3</sup>) at evaluation sites for final models shown in Tables S3 and S5



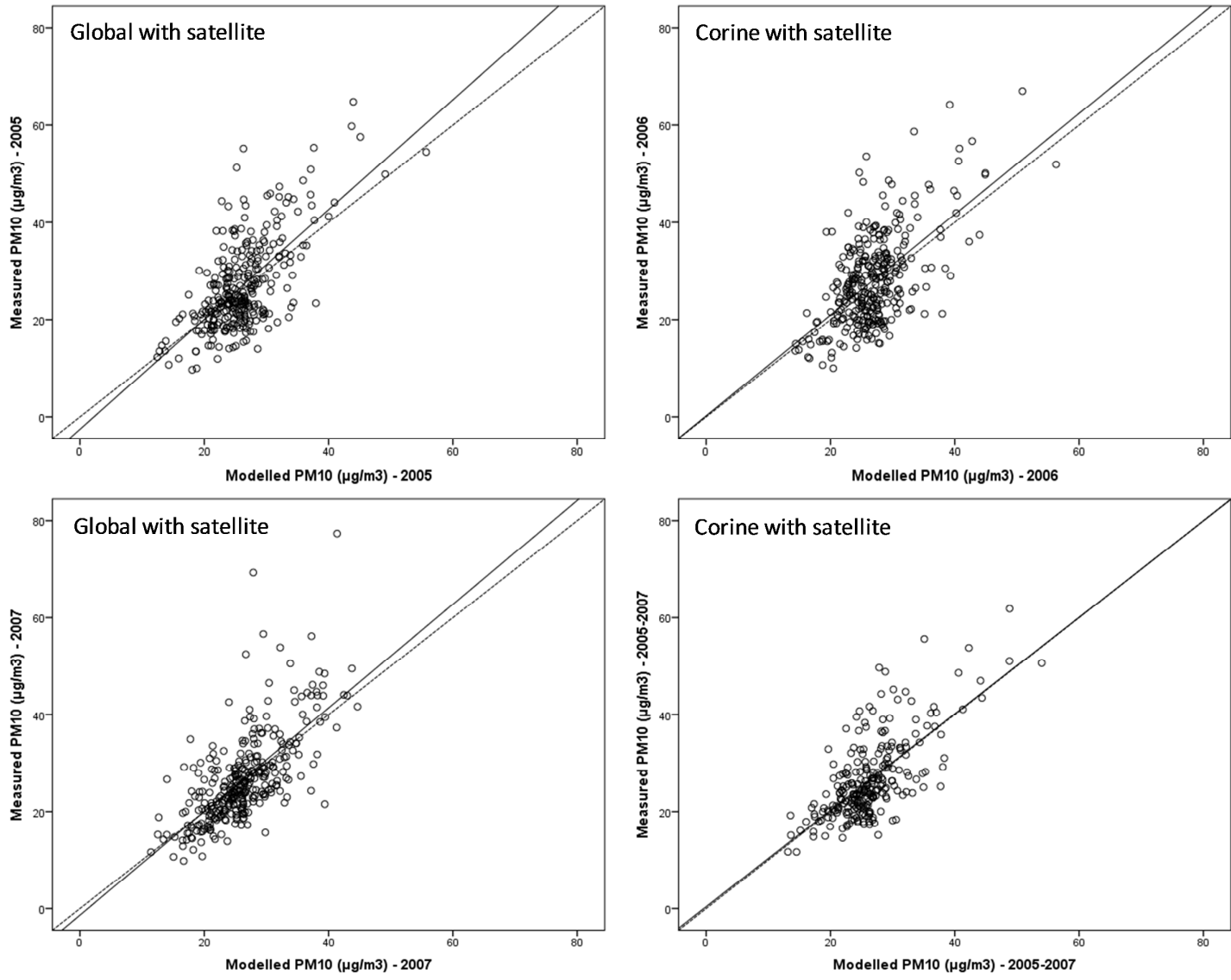


Figure S6. Modelled vs. measured PM<sub>10</sub> concentration ( $\mu\text{g}/\text{m}^3$ ) at evaluation sites for final models shown in Tables S4 and S5